THE SOLID WOOD FILLED TUBE UNDER AXIAL LOADING

TEO KAH CHUN

UNIVERSITI TEKNIKAL MALAYSIA MELAKA

THE SOLID WOOD FILLED TUBE UNDER AXIAL LOADING

TEO KAH CHUN

This report is submitted
in fulfillment of the requirement for the degree of
Bachelor of Mechanical Engineering (Structure and Materials)

Faculty of Mechanical Engineering

UNIVERSITI TEKNIKAL MALAYSIA MELAKA

2017

DECLARATION

I declare that this project report entitled "The Solid Wood Filled Tube Under Axial Loading" is the result of my own work except as cited in the references

Signature : ....

Name : ....

Date : ....

APPROVAL

I hereby declare that I have read this project report and in my opinion this report is sufficient in terms of scope and quality for the award of the degree of Bachelor of Mechanical Engineering (Structure & Materials).

Signature : ....

Supervisor's Name : ....

Date : ....

DEDICATION

To my beloved mother and father

ABSTRACT

Efficient energy absorbers are widely made from thin-walled structures such as aluminium because of the good energy absorption capacity. In this paper, the behavior of hollow tubes and wood-filled tubes that subjected to axial loading in quasi-static test is studied. Agarwood which known as "Gaharu" would be the wood that been used in this study. To this aim, quasi-static axial loading test have been performed on square and circular aluminium tube. Experimental work showed the effect of solid wood for the energy absorption capacity of tubes. The mode of deformation for the circular tube and square tube is investigated. Results from the quasi-static test are presented on tubes of various length which consisted of 50mm, 100mm, 150mm and 200mm. Theoretical models of axial collapse modes for circular tube and square tube has been developed and established a comparison between theoretical results and experimental results. The results obtained for the mean load and plastic wavelength agreed reasonably with the experimental observations. Satisfactory agreement were generally achieved between theoretical value and experimental value of mean load and plastic wavelength. In this paper, it also highlighted the comparison of square tube and circular tube in terms of energy absorption and specific energy absorption. The energy absorption in wood-filled tube is shown to be higher than the hollow tube whereas the specific energy absorption in hollow tube is shown to be higher than wood-filled tube. Some observations are made on the influence of geometrical imperfection and the methods to reduce the deviation of theoretical value and experimental value.

ABSTRAK

Penyerap tenaga yang cekap diperbuatkan daripada struktur berdinding nipis secara meluas seperti aluminium kerana mempunyai kapasiti penyerapan tenaga yang baik. Dalam laporan ini, ciri-ciri tiub berongga dan tiub dipenuhi kayu yang dikenakan pembebanan paksi dalam ujian kuasi-statik akan dikaji. Kaya gaharu akan digunakan dalam kajian ini. Untuk mencapai matlamat ini, ujian statik beban paksi telah dilakukan ke atas tiub aluminium persegi dan bulat. Eksperimen menunjukkan impak daripada kayu yang kukuh kepada kapasiti penyerapan tenaga tiub. Cara ubah bentuk untuk tiub bulat dan tiub persegi telah dikaji. Keputusan ujian kuasi-statik yang ditunjukkan adalah pada tiub yang terdiri daripada pelbagai kepanjangan seperti 50mm, 100mm, 150mm dan 200mm. Model teori untuk mod kejatuhan paksi untuk tiub bulat dan tiub persegi telah dibangunkan dan mewujudkan suatu perbandingan antara keputusan teori dan keputusan eksperimen. Keputusan yang diperolehi untuk beban purata dan kepanjangan plastik gelombang adalah munasabah dengan pemerhatian daripada eksperimen. Persetujuan yang memuaskan pada umumnya dicapai antara nilai teori dan nilai eksperimen beban purata dan kepanjangan plastik gelombang. Dalam laporan ini, ia juga menekankan perbandingan tiub persegi dan tiub bulat dari segi penyerapan tenaga dan penyerapan tenaga tertentu. Penyerapan tenaga dalam tiub dipenuhi kayu ditunjukkan lebih tinggi daripada tiub berongga manakala penyerapan tenaga tentu dalam tiub berongga ditunjukkan lebih tinggi daripada tiub dipenuhi kayu. Beberapa pemerhatian yang dibuat ke atas pengaruh ketidaksempurnaan geometri dan kaedah untuk mengurangkan penyelewengan nilai teori dan nilai eksperimen.

ACKNOWLEDGEMENTS

I would like to acknowledge with much appreciation the crucial role of Prof. Dr Md Radzai bin Said, who gave permission for me to complete my final year project under his supervision. He is willing to teach patiently and guide me well in these two semesters of my final year project. He gives a lot of advices and encouragement to lead me to a correct way to complete my project.

Next, a special thanks goes to the laboratory technician, Encik Faizol bin Kamarul Zahari for his willingness and kindness to help me during my experimental work. Without the aid from them, I believe that I am not able to finish my experiment with the satisfied results. They are very efficient as they manage to help us arrange the schedule to use the laboratory in a short time.

Last but not least, many thanks go to my course mates. Throughout these two semesters, we are giving supports and help to each other. I am very appreciate with their full effort of helping when I am encountered with problems.

Finally, I would like to express my gratitude towards my parents for their kind encouragement which help me in completion of this project. With their supports, finally I am able to complete my project smoothly.

TABLE OF CONTENTS

LIST OF TABLES

LIST OF FIGURES

LIST OF ABBEREVATIONS

ASTM	American Society for Testing and Materials
AutoCAD	Auto Computer Aided Design
kPa	kiloPascal
MPa	MegaPascal
GPa	GigaPascal
UTM	Universal Testing Machine
LED	Light Emitting Diode
J	Joule
kJ	kiloJoule
kg	kilogram
N	Newton

LIST OF SYMBOLS

D	=	Diameter
t	=	thickness
Y	=	yield strength
H	=	tube length
E	=	modulus of elasticity
σ	=	sigma
A	=	cross sectional
P	=	magnitude of load
P_{max}	=	initial phase peak load
P_{ij}	=	maximum and minimum load
P_m	=	mean or average load
EA_i	=	energy absorptions quantity
H	=	plastic half fold length
h	=	thickness
M_o	=	fully plastic bending moment per unit length
n	=	number of lobes
c	=	side length

LIST OF APPENDICES

CHAPTER 1

INTRODUCTION

1.1 Background

Nowadays, safe design of components and systems is an important issue in our community. This is due to the purpose of decreasing the human suffering as well as the financial burdens on society. One of the awareness that increased among public is what can be done in order to reduce the potential danger of impact dangers. One of the many types of tragedies like vehicle crash, the occupant safety is the main concern. So, the vehicle structures need to be designed well, acted as collision safety protection to absorb and dissipate the direct impact force (Alghamdi, 2001). Thin-walled structures are widely used in the crashworthiness application such as automotive and aeronautical to withstand the impact force (Liu et al., 2015). An energy absorber is a system that transform, fully or partially, kinetic energy into another form of energy. Thin-walled structures are good energy absorber due to the impressive folding deformation during axial compression (Alavi Nia and Parsapour, 2014). Techniques of applied load, transmission rates, deformation patterns and material properties are the dependent variables for the conversion of kinetic energy into plastic deformation (Johnson and Reid, 1978). In addition, thin-walled structures are light weight, economic, high ductility and ease of manufacture. Since long time ago, there are many researchers had done the studies on how to enhance the energy absorbance and dissipation during crash via changing material characteristic, geometry and type of filler.

Generally, there are various types of absorbers that been used such as tubular rings, circular tubes, square tubes, corrugated tubes, honeycomb cell and so forth. Under the quasi-static loadings, the square tube and circular tube will be collapsed in either concertina, diamond or mixed mode. Basically, there are divided into seven categories such as sequential concertina, sequential diamond, Euler, concertina and diamond, simultaneous concertina, simultaneous diamond and tilting of tube axis (Andrews et al., 1983).

For these thin wall tubes, the filler such as solid wood can be combined with the tubes to stabilize and minimize the probability of the tubes to undergo Euler type of buckling. For the square tubes and circular tubes that filled with solid wood, it has been proved that the solid wood is able to increase the stability of the tubes (Lampinen and Jeryan, 1982).

This is because the filling of solid wood enable the tubes to undergo higher plastic deformation and higher energy absorption (Duarte et al., 2015).The solid wood is able to decrease the half-wavelength of the elastic buckling mode to values nearer to plastic fold lengths. Therefore, the energy absorption capacity can be enhanced by eliminating the non-compact mode (Reddy and Wall, 1988).

The solid wood filled tube and the empty tube will be compared in terms of the peak load, mean plastic half wavelength, energy absorption and the buckling mode (Florence et al., 1991). The energy absorption of the empty square tube and circular tube is roughly half of the energy absorption of the solid wood filled tube (Reid and Reddy, 1986). It is known that the interaction between the solid wood and the tube can provide a maximum benefit when there is an optimum combination (Reid et al., 1986).

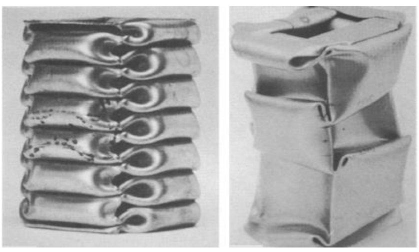

Figure 1.1 Axially crushed square tube in compact and non-compact mode (Reddy and Al-Hassani, 1993)

1.2 Problem Statement

The impact of transport vehicles is an unfortunate but common occurrence. It is becoming apparent that, in the future, transport structures will have to be designed to withstand impact and crashes. The current trend in producing lighter structures but puts greater demands on the designer since more aspects of design become critical as the weight is reduced, and working stresses become closer to the ultimate strength of the material. In the case of crash or impact, the requirement is achieved through properly designed high absorption system. Thin-walled structure is always a good energy absorber but there is still insufficient to sustain the huge impact that acted upon it sometimes. So, the combination of the filler such as solid wood with the tube is able to increase the energy absorption and prevent the happening of fatal accident.

1.3 Objectives

The objectives of this project are as follows:

1. To observe and study the deforming mode of empty and filled tube under axial loading
2. To determine the plastic wavelength and compare with theory
3. To study the load-displacement characteristics and lead to energy absorption

1.4 Scope of Project

The experimental project will focus on the empty and wood filled circular and square tube that will be compressed. The mode is compared between quasi-static with various length of tube with only one type of local wood. The deforming mode, plastic folding, mean load and densification and energy absorbed will be observed. INSTRON quasi-static is used to perform experimental. Previous analytical work will be compared. Particularly in Euler Global bucking is searched and observed. Compression of wood alone is also performed.

CHAPTER 2

LITERATURE REVIEW

2.1 Introduction

This literature study is to find the relevant information that related on the solid wood filled tube under axial loading. The criteria that included in this chapter are energy absorber, deformation mode of empty tube, solid wood, uniaxial loading and mechanical properties.

2.2 Energy Absorber

Energy absorber is a device that able to absorb energy due to impact and dissipate it in other form of energy which is ideally in an irreversible manner. An energy absorber should be light in weight and able to keep the maximum allowable retarding force the same with the greatest displacement. Tubes that will buckle in the progressive manner when subjected to axial compression is providing a cheap and good energy absorbing capacity (Jones, 2012).

Circular and square shape tubes are frequently preferred as energy absorber due to their common occurrence and easy manufacturability. For example, circular tubes can dissipate elastic and inelastic energy through different modes of deformation which show the different response of energy absorption. Lateral compression, lateral indentation, tube splitting, tube inversion and axial crushing are the examples of the methods of deformation.

Nowadays, mostly all of the transportation are designed with thin-walled component. The structure components of vehicles must withstand the huge loading or impact during various kinds of accident to meet stringent integrity requirements. For instance, accidents are happened either motorcycles, car or aeroplane, the design of the passenger seat must able to withstand the crash force that acted upon it without immoderate deformation that harmful to the passengers. Also, the barrier that located at the road side must be able to dissipate impact energy in controlled manner that ensure the deceleration level is under the safety limit of the vehicles. In addition, thin-walled structures are widely used in the designing of vehicles for air, sea and land (Abramowicz, 2003).

An efficient crush elements will be produced when a combination of tubular members and cellular filler material occurs. This because they are combining cooperatively the advantages of both types of structures. It will be seen the enhancement of energy absorption when compared to empty tubes due to the interaction effect between tube and filler. The interactions will lead to the changing of buckling modes and lead to higher energy dissipation of tube. The filler material helps to increase the efficiency of energy absorbing by changing the irregular pattern of buckling modes (Seitzberger et al., 2000).

2.3 Deformation Mode of Empty Tube

2.3.1 Circular Tube

Axial crushing of metallic tubes has been the subject of extensive research. Circular shapes might provide the widest range of all choices for use as absorbing elements because of their favourable plastic behaviour under axial forces, as well as their common occurrence as structural elements. (Aljawi, 2002).

For the circular tube, the axial crushing under quasi-static loading is classified to seven different categories such as sequential concertina, sequential diamond, Euler, concertina and diamond, simultaneous concertina, simultaneous diamond and tilting of tube axis. It is studied that the small D/t ratio of thick cylinder which ranges from 80 to 90 will buckle in the concertina which is axisymmetric mode meanwhile thin cylinders with high value D/t ratio will occur buckling in the diamond which is deformation of non-axisymmetric mode. For deformation of diamond, the lobes will increase along with the increase of D/t ratio (Andrews et al., 1983).

Diamond mode of deformation expresses a lower energy absorbing capacity than the mode of concertina which is lesser of D/t ratio. The transition point where the concertina mode transforms to diamond mode at about D/t = 100. The transition point will be depend on the ratio of yield strength and modulus of elasticity, Y/E. In a larger value of Y/E with smaller value of D/t ratio, the changes of transition to concertina mode will occur (Pugsley, 1978). The circular tube that been used in the experimental work is shown in Figure 2.1.

Figure 2.1 Circular aluminium tube

2.3.2 Square Tube

For the square tube, the deformation of progressive folding occurs when the ratio of thickness to the side length is bigger than 0.025 (Abramowicz and Jones, 1984). This shows the tube length is exhausted with a sequence of contiguous fold. The effect of strain hardening will cause the original length 2H of a particular mechanism to be reduced to 75% of original value when fully crushed (Abramowicz, 1983).

In order to improving the energy absorption capacity, the elimination of non-compact mode should be done by reducing the half-wavelength of elastic-wavelength to the amount that nearer to plastic fold lengths (Reid et al., 1986).

There are two types of deformation which is compact mode and non-compact mode. Compact mode is defined when contiguous fold occurs since one end of the tube start to occur progressive buckling. This is different with the non-compact mode occurs at thinner tube in which the fold mechanisms are apart to each other where the distance is about the side length of tubes. Non compact mode has lower specific energy thus will cause the happening of global instability which is Euler failure mechanism (Thornton et al., 1983). The square tube that been used in the experimental work is shown in Figure 2.2.

Figure 2.2 Square aluminium tube

2.4 Solid Wood

Solid wood is the predominant material comes from all the species of trees. It is just similar to a rigid, closed cell foam. This defines that it can be crushed with sufficient energy and absorb the significant energy. For sure different species of wood will show different properties and even few samples of wood that in the same species of wood will probably show a different behaviour. In fact, almost any types of the solid wood has a better capability in absorbing more energy than the types of solid plastics that typically used in the market.

The response of Agarwood when it is applied by a force is dependent on the orientation of the piece's grain. In a typical tree, there are three types of grain such as transverse, radian and end grain. These three types of grains indicate the "lay" pattern of the wood cell. For example, Agarwood is compressed directly on the end grain will react differently from the same piece of Agarwood that compressed on the transverse grain. End grain responds with cracking but radial and transverse responds by going to crush. Actually in both this case represent the same behaviour of absorption of impact energy.

In the market, there are some solid woods that very resilient and dense. It means that they will not be easily crushed or cracked. They able to perform high durability in mechanical applications like impacts. There are two types of solid wood which are hard wood and soft wood. Basically, Agarwood is a soft wood that will crush and crack more readily because they are less dense and resilient than hard wood which provide more capacity to absorb the energy of huge impacts. Both types of solid wood are actually able to perform better in the absorption of the impact energy. Solid wood is good in absorbing impact energy. It acts as a good protection over a greater spectrum of impact energies (Bucur, 2006).

2.4.1 Deformation of Solid Wood Filled Tube

It has been studied that the circular tube and square tube can be stabilized by filling them with a crushable medium like solid wood (Lampinen and Jeryan, 1982). It is known that the type of the filler is very important as it has to interact with the tubes in order to enhance the energy absorption capacity. A higher density of fillers basically able to increase more the energy absorption capacity. There is an optimum combination where interaction between the filler and tube produce a maximum benefit (Reid et al., 1986).

So, a low strength of solid wood in strong tubes cause a minor effect while high strength solid wood in weak tubes will cause the rupture happened and affect the performance of the system. It is indicated that the performance of the system is mainly due to how is the interaction between solid wood and tube. The effect of solid wood in the tubes will decrease the half-wavelength of the elastic buckling mode to values nearer to plastic fold lengths. Therefore, energy absorption capacity can be improved by eliminating the non-compact mode. (Reddy and Wall, 1988)

2.5 Uniaxial Loading

Stress is occurred on the structure which defined as the force per unit area, or intensity of the forces distributed over a given section. It is also denoted by the Greek letter σ (sigma). According to Eq. (2.1), the stress in a member of cross sectional, A subjected to axial load P is obtained by dividing the magnitude P of the load by the area A:

$$\sigma = \frac{P}{A} \tag{2.1}$$

When the member is in tension, it will show a positive sign that indicates tensile stress while member in compression will show a negative sign which indicates the compression test. The SI metric units will express axial load, P in newtons (N), area, A in square meters (m^2) and stress, σ in N/m^2. This unit is known as Pascal (Pa). According to Eq. (2.2), there are few types of units been used in practice which are kiloPascal (kPa), MegaPascal (MPa) and GigaPascal (GPa). (Beer et al., 2009)

$$
\begin{aligned}
1\ \text{kPa} &= 10^3\ \text{Pa} = 10^3\ \text{N/m}^2 \\
1\ \text{MPa} &= 10^6\ \text{Pa} = 10^6\ \text{N/m}^2 \\
1\ \text{GPa} &= 10^9\ \text{Pa} = 10^9\ \text{N/m}^2
\end{aligned}
\tag{2.2}
$$

2.5.1 Axial Compression

The response of axial compression for thin-walled structure which is ductile metallic alloy elements is widely studied for the potentiality of absorbing energy in irreversible manner. Axial compression plays an important role in the engineering field especially in crashworthiness and blast-resistant design of structures.

Axial compression is consisted of few phases or stages. The two phases are categorized into first phase and second phase. In first phase the response of the pre-collapse will be determined. By referring to the Figure 2.3, the happening of the maximum load, transformation of sidewalls from the axial to bending load-resistance, formation of folds of the early few interior and exterior on the sidewalls which shows increment and decrement in the load-displacement curve. Steady state fold formation process is the secondary folding phase. In this phase, there will be a formation of fixed wavelength due to the interaction at adjacent sidewall along the leftover length of the specimen (Dipaolo and Tom, 2006).

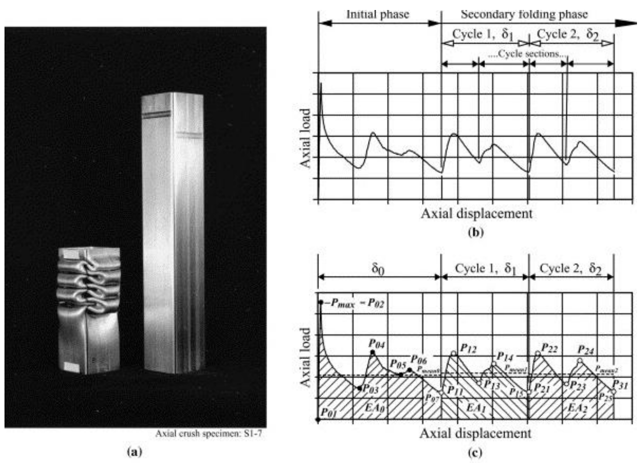

Figure 2.3 Curve sections of initial phase and secondary (Dipaolo and Tom, 2006)

Comparison and evaluation of performance for components is done with the terms "crush characteristic" which is direct data and derived quantities. This includes the direct data and derived quantities. The direct data that obtained from the load-displacement curve is the initial phase peak load, P_{max} maximum and minimum load, P_{ij} mean or average load, $P_{min,}$ energy absorptions quantity, $EA_{i,}$ axial displacement, δ_i. Changes mode from fold formation of ductile to fracture will be studied. The difference of the load-displacement graph and the fold formation process will cause the evaluation of strong plastic deformation of phase characteristics and material details cannot be conducted. The evaluation for characteristic of phase cannot be conducted due to the not similarity of fold formation process and shapes of load-displacement graph. (Karman, 1941)

2.5.2 Quasi-Static Test

In quasi-static testing, material elasticity is unimportant because of the extensive plastic deformation. When the plastic energy dissipated in the structure is larger than three times the elastic of deformation, the elastic effect will be neglected. Besides, from an energy point of view, the initial buckling response of structures under quasi-static is less important than the subsequent post-buckling, yielding behaviour, which associated with large strains and deflections. This behaviour will be assumed as rigid-plastic model because the energy absorbed in the elastic deformation is usually unimportant. Studies have done on the transition of the axially crushed tubes from the Euler (global) bending mode to the progressive buckling mode at static and dynamic loading conditions. This transition point much depends on the length of tube, cross section, material type, strain-hardening, strain rate and end conditions. Global buckling may or may not coincide with the maximum load-carrying capacity of the column. Quasi-static is acceptable at low impact velocities which usually ignore the inertia effect. The axial crushing of tubes under quasi static condition are categorized into seven categories such as sequential concertina, sequential diamond, Euler, concertina and diamond, simultaneous concertina, simultaneous diamond and tilting of tube axis (Alghamdi, 2001).

2.6 Mechanical Properties

2.6.1 Tensile Testing

Tensile testing that known also as tension test can be said the most fundamental type of mechanical test that performed on material. Tensile test does not has the complicated procedures to carry on and relatively inexpensive and fully standardized. One material property that is widely used and recognized is the strength of a material. Therefore, what is meant by the strength of material will be indicated by tensile test through the lots of mechanical behaviour that provided by it.

The basic concept of tensile test is by putting a specimen between two fixtures known as "grips". The cross sectional area including length, width and thickness must be determined before conducting the test. The load or force will be applied on one end while other end is fixed. As the specimen is being pulled, strength of material can be known along with how much it elongates. After the specimen breaks, the mechanical properties can be determined such as yield strength, ultimate strength, maximum elongation and Young's Modulus. The main outcome of tensile test is a graph of stress versus strain that converted from a graph of load versus elongation. Since both the engineering stress and the engineering strain are obtained by dividing the load and elongation by constant values of geometry information, the load-elongation curve will have the same shape as the engineering stress-strain curve (David, 2004).

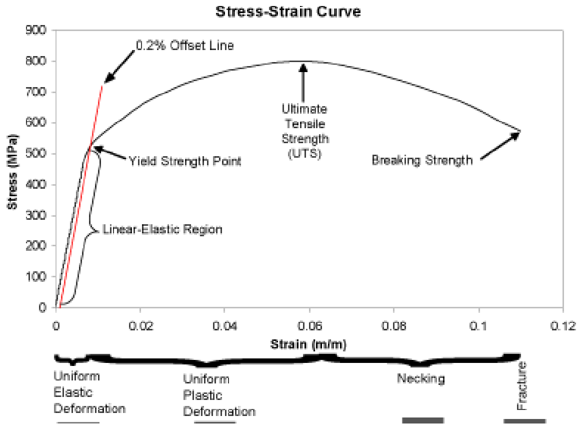

Figure 2.4 Graph of stress versus strain (NDT Resource Center, n.d.)

2.6.2 Yield Strength

Yield strength is act as a point at which a material starts to deform plastically. The material will return to its original length once released from applied force when it is not yet reaching the yield point. This condition is known as elastic deformation. Once the yield point is reached, some fraction of deformation will be permanent and non-reversible. A yield surface will be formed from an infinite number of yield point if it is in three-dimensional principal stresses. Yield strength acts as a limit of performance for mechanical structures since it indicates the upper limit to force that can be applied without permanent deformation. In structural engineering, it is considered as a soft failure mode since it will not cause a disastrous failure unless it accelerates buckling. Yield strength is one of the significant mechanical properties in various types of material-working such as reshape material with pressure, cutting to split material or shearing and assemble component tightly with fasteners (Beer et al., 2009).

2.6.3 Ultimate Strength

Ultimate strength which also known as tensile strength. It is referred to the capacity of a component or structure to withstand loads tending to elongate which opposed to the compression strength which is strength of opposing the loads to reduce size. In short, tensile strength resists the tension force that applied on the material. Ultimate tensile strength which means the maximum stress of the material can withstand with when stretching or pulling before fracture.

Ultimate strength of a material or structures is determined by performing tensile test and obtained from the graph of stress versus strain. The value of ultimate strength is independent form the size and dimension of the shape since it is an intensive property. But, it may dependent on other factors such as preparation of specimen, presence of flaw or defect, and of course the environment condition.

Ultimate strength is measured in pascal (Pa) which force per unit area since it is defined as stress. (Beer et al., 2009)

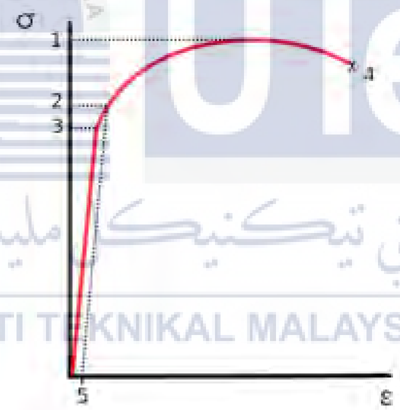

Figure 2.5 Point 1 is indicated as ultimate strength (Zaborski, n.d.)

2.6.4 Young's Modulus

Young's Modulus is a mechanical property of a linear elastic material that determine the stiffness of a material. It shows the relationship of stress and strain in a material. The deformation of a stiff material that requires a higher force that acting upon it and it is assumed to be a perfectly rigid material when there is an infinite force. These conditions show that this material has an infinity value of Young's Modulus.

Young's Modulus is the ratio of stress to strain where strain is dimensionless. So, it has units of Pascal (Pa). It is applicable in calculating the dimension change on a material where the tension or compression load is applied on it. For example, it helps to determine the elongation of material during tension or the contraction during compression occur. When it is directly applied to uniaxial stress case, the tension or compressive stress is occurred in single direction only (Beer et al., 2009)

2.7 Theoretical Model for Circular Tube

The deformation of a circular tube that compressed under axial load is classical problem in solid mechanics. It is found that the energy absorption capacity of circular tube is one of the best devices. It has a comparatively high energy absorption capacity because it supplies a reasonably constant operating force. In study of static crushing of structures, material elasticity is not important because of the extensive plastic deformation. Therefore, the elastic energy will be neglected when the plastic energy dissipated in the structure is larger than three times the elastic energy of deformation. (Alghamdi, 2001). The circular thin walled structure will collapse either axisymmetrically or non-symmetrically when it is crushed axially. It is depending on the ratio of diameter and thickness (D/h). The axisymmetric mode which is also known as ring mode or concertina mode while non-symmetrical mode is known as diamond mode. For certain D/h, a tube might deformed with concertina mode and then switch to diamond mode, so exhibiting a mixed mode. The diamond mode occurs when the D/h is greater than 80. For D/h less than 50, the ring mode is present for L/h less than 2 and a mixed mode for L/h larger than 2. Euler-type buckling takes place for long tube.

In a typical load-displacement curve, the axial force reaches an initial peak and followed by a sharp drop and then fluctuations. These are a result of formation of successive folding; each subsequent peak corresponds to the onset of a folding process. Sometimes, there is a secondary peak in between two successive peaks. The energy absorbed is simply the area under this curve. For practical purposes, the average force is often worked out as an indication of energy-absorption capacity.

The first person that gave a theoretical model for the crushing of circular tube for ring mode in axial direction is Alexander. The model is shown in Figure 2.6 and Figure 2.7.

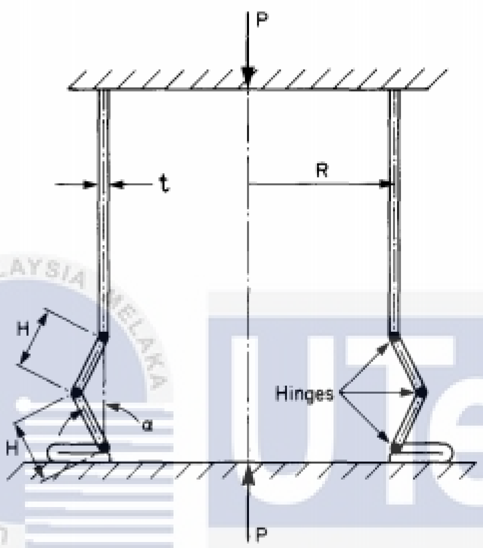

Figure 2.6 Simple theoretical model for axisymmetric collapse (Alexander, 1960)

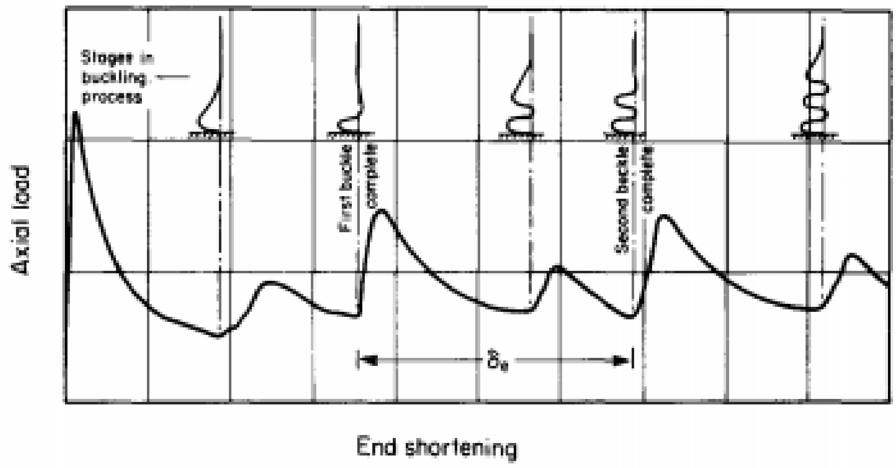

Figure 2.7 Relationship between generator shape and shape of load-deflection curve for axially symmetric buckling mode (Alexander, 1960)

In this model, there are three circumferential plastic hinges formed during the formation of single fold. The plastic hinges will experience circumferential tensile strain when the assumption that fold goes completely outwards is made. Plastic bending of the three hinges dissipate the external work done and circumferential stretching of the materials in between. According to Eq. 2.3, unknown length of H is obtained by citing the idea that the value of H is the external force P_m is minimum.

$$H = 0.95\sqrt{Dh} \tag{2.3}$$

According to Alexander analysis, the material will be deformed partially inwards and partially outwards. So, the average load can be taken as Eq. 2.4,

$$P_m \approx 6Yh\sqrt{Dh} \tag{2.4}$$

Johnson (1972) has done some modifications on Alexander Model with expression for the stretching energy on the grounds that the circumferential strain varies along s. It was identified that the tube will be deformed with wall bends in the meridian direction instead of straight line (Abramowicz, 1983; Abramowicz and Jones, 1984b and 1986). In their model, the effective crush length is considered which is smaller than 2H. Thus, a little bit higher mean load will be obtained and equation will be shown in Eq. 2.5,

$$P_{m=}8.91Yh\sqrt{Dh}(1 - 0.61\sqrt{\frac{h}{D}} \tag{2.5}$$

Theoretical model for diamond mode is not as victorious as the ring mode. Pugsley and Macaulay (1960) were the first investigator to study diamond mode. They proposed Eq. 2.6,

$$\frac{P}{Y\pi Dh} = 10\frac{h}{D} + 0.13 \qquad (2.6)$$

Johnson et al. (1977b) tried to develop a theory for diamond mode according to the experiments with PVC tubes. A given number of lobes can be worked out from the arrangement of hinge lines. The arrangement of three lobes is shown in Figure 2.8.

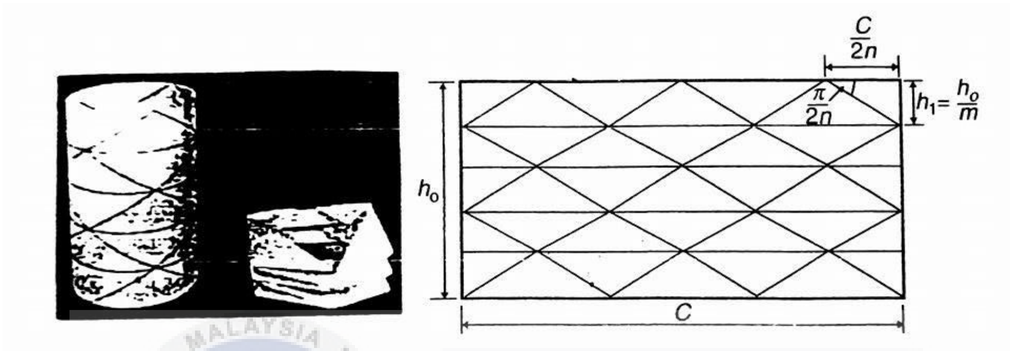

Figure 2.8 A theoretical collapse model for non-symmetric mode; n=3 (Johnson et al., 1977b).

Further theoretical studies were carried out by Singace (1999). An eccentricity factor was recognized in the same method for the ring mode. The equation 2.7 developed is

$$\frac{P_m}{M_o} = -\frac{\pi}{3}\mathrm{n} + \frac{2\pi^2}{n}\tan\left(\frac{\pi}{2n}\right)\frac{D}{\mathrm{h}} \qquad (2.7)$$

2.8 Theoretical Model for Square Tube

Thin-walled square tubes are often subjected to axial loads. They are representative of a number of structural components in, for example, cars, railway coaches and ships. The collapse mode of square tube is different with circular tube, but the general behavior of load-displacement curve is similar. Both of square tube and circular tube undergo progressive collapse when subjected to axial loading. A common load-displacement curve is plotted in

Figure 2.9. The tube wall of a typical square tube that being crushed fully is shown in Figure 2.10. It undergoes severe inward and outward plastic bending with possible stretching. For non-compact mode, the fold is separated by distance about equal to the side length of tube as shown in Figure 2.11. (Reid et.al., 1986).

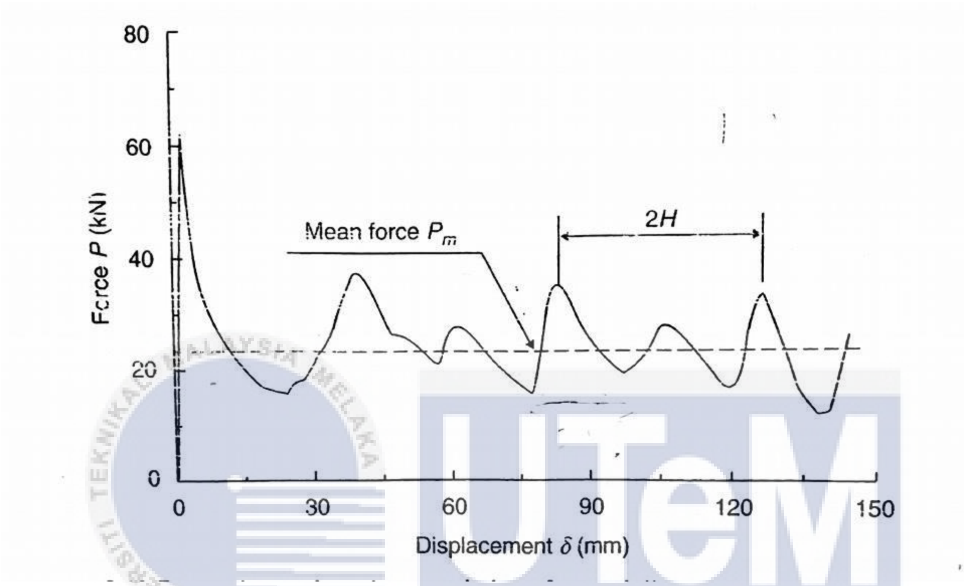

Figure 2.9 Force shortening characteristics of an axially compressed thin-walled aluminum column (Reid et al., 1986)

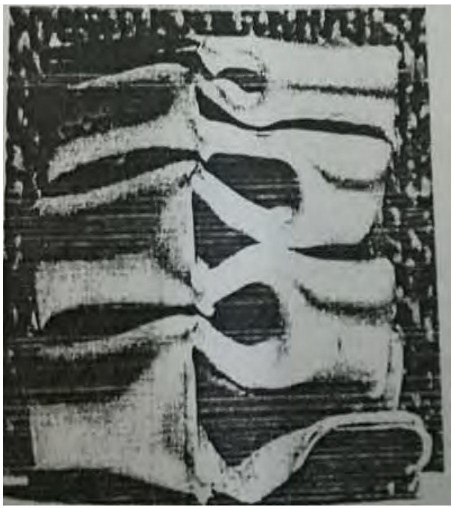

Figure 2.10 Compact mode (Reid et al., 1986)

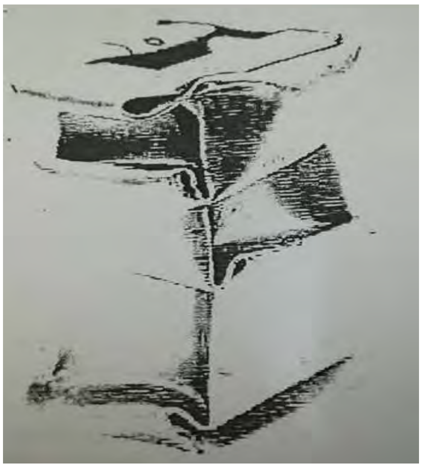

Figure 2.11 Non-compact mode (Reid et al., 1986)

According to Eq. 2.8, the plastic half fold length is

$$H = 0.983\sqrt[3]{hc^2} \tag{2.8}$$

Based on Eq, 2.9, the mean load for square tube is

$$P_m = 9.56Y h^{\frac{5}{3}} c^{\frac{1}{3}} \tag{2.9}$$

P_m is directly proportional to $h^{\frac{5}{3}}$ is a reflection of the energy contribution of bending and stretching.

CHAPTER 3

RESEARCH METHODOLOGY

3.1 Introduction

This chapter describes the methodology for the experiment work of solid wood filled tube under axial loading. This methodology is to make sure the work flow of this study is going on smoothly and systematically. In the Figure 3.1 shown below, it shows the systematic process which are important steps that need to be emphasized on. The process includes literature study, determination of material, fabrication of specimen, develop tensile test, analysis of tensile test result, develop compression test, analysis of compression test result, preparation of final report and submission of final report. The Gantt chart for this study can be seen at APPENDIX A1 and APPENDIX A2.

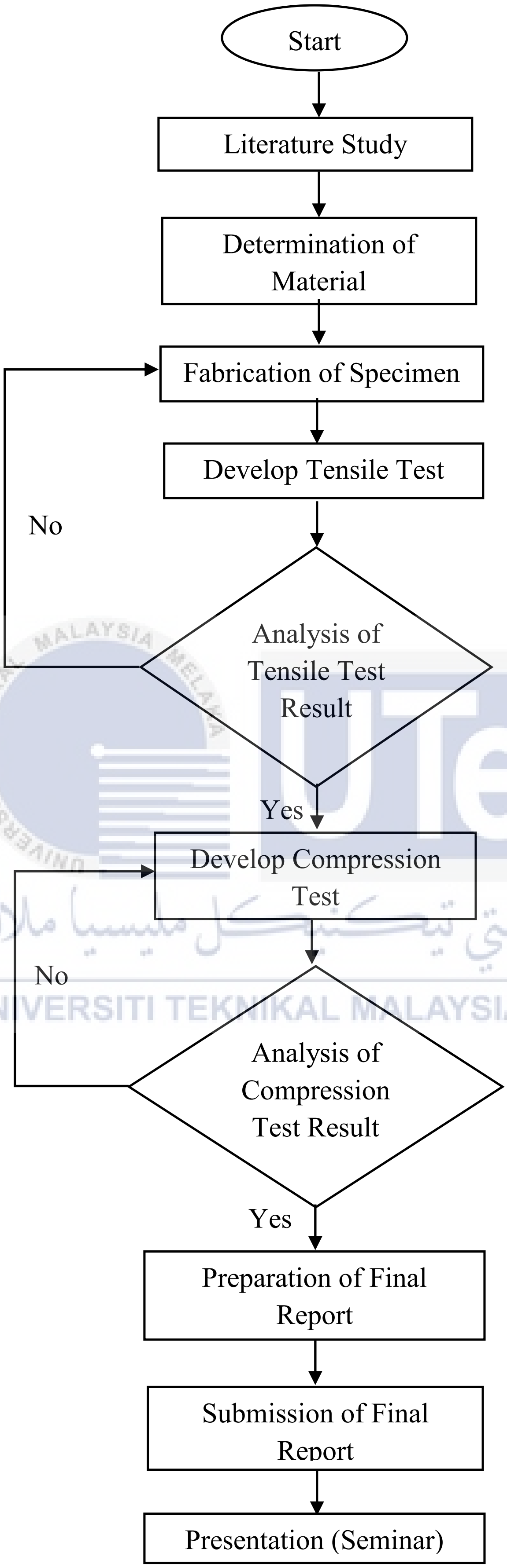

Figure 3.1 Flow chart of methodology

3.2 Determination of Material

First of all, the types of material was chosen which is aluminum tube after getting a short brief from supervisor. The shape of aluminum tubes are decided as circular shape and square shape. These two shapes of tubes will be the specimen for the experimental work.

In the storage area which located in Makmal Fasa B, there were many type of aluminum tubes with different dimensions and shapes. At last, the materials were chosen and their dimensions were measured by using the Vernier caliper. The dimension of the materials were shown in the Table 1 and Table 2 that shown below. For the square tube, the side length is 44.65 mm whereas the thickness is 1.35 mm.

Table 3.1 Dimension of square tube

Parameter	Dimension
Side length	44.65mm
Thickness	1.35mm

Figure 3.2 Square aluminum tube

For the circular tube, the side length is 44.65mm whereas the thickness is 1.35mm.

Table 3.2 Dimension of circular tube

Parameter	Dimension
Outer Diamter	25.3mm
Thickness	1.5mm

Figure 3.3 Circular aluminum tube

3.3 Fabrication of Specimen

After the determination of material, the following steps was the fabrication of specimen for tensile testing. Tensile testing is conducted to determine the mechanical properties of aluminum tubes.

3.3.1 Laser Cutting Machine

Based on the requirement of ASTM E8 which is the standard test methods for tension testing of metallic materials, the specimens for conducting the tension test need to be in a specific shape, like a “dog bone” shape.

In order to fabricate the specimens for tensile test, laser cutting machine was used. As per requirement of the laser cutting machine, the drawing of the tensile test specimen need to be drawn by using AutoCAD software. Therefore, drawing was constructed by using AutoCAD version 2008 according to the ASTM E8 standard. The dimensions of the tensile test specimens were shown in Figure 3.3 as below:

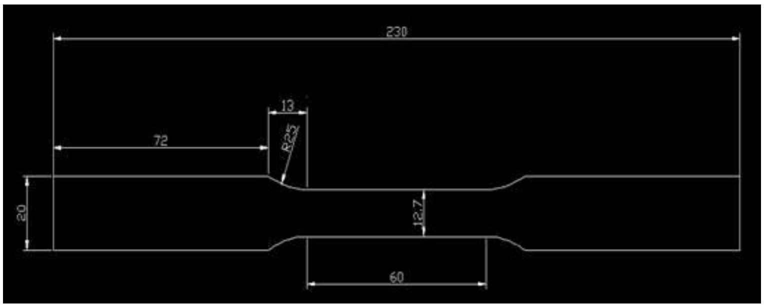

Figure 3.4 Dimensions of tensile test specimen

The dimensions of tensile test specimen above were referred in the Table 1 that shown below. It is the standards of the specimens in the sheet-type form.

Table 3.3 Standards for Sheet-type tension test material (ASTM, E8, 2001)

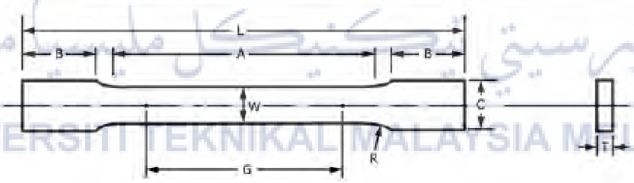

Dimensions	Standard Specimens		Subsize Specimen
	Plate-Type, 40 mm [1.500 in.] Wide	Sheet-Type, 12.5 mm [0.500 in.] Wide	6 mm [0.250 in.] Wide
	mm [in.]	mm [in.]	mm [in.]
G—Gauge length (Note 1 and Note 2)	200.0 ± 0.2 [8.00 ± 0.01]	50.0 ± 0.1 [2.000 ± 0.005]	25.0 ± 0.1 [1.000 ± 0.003]
W—Width (Note 3 and Note 4)	40.0 ± 2.0 [1.500 ± 0.125, -0.250]	12.5 ± 0.2 [0.500 ± 0.010]	6.0 ± 0.1 [0.250 ± 0.005]
T—Thickness (Note 5)		thickness of material	
R—Radius of fillet, min (Note 6)	25 [1]	12.5 [0.500]	6 [0.250]
L—Overall length, min (Note 2, Note 7, and Note 8)	450 [18]	200 [8]	100 [4]
A—Length of reduced parallel section, min	225 [9]	57 [2.25]	32 [1.25]
B—Length of grip section, min (Note 9)	75 [3]	50 [2]	30 [1.25]
C—Width of grip section, approximate (Note 4 and Note 9)	50 [2]	20 [0.750]	10 [0.375]

3.3.2 Disc Cutter Machine

The disc cutter machine was used to cut the aluminum tubes into 600mm length. Based on the experience from the technician for laser cutting machine, it was assumed that four tensile test specimens could be cut for the 600mm long of aluminum tubes. Safety precaution was done by wearing goggles and mask when cutting the aluminum tubes.

3.4 Develop Tensile Testing

Tensile test was conducted in order to determine the mechanical properties of aluminum. The four main mechanical properties that must be found are ultimate strength, yield strength, maximum displacement and Young's Modulus. The Figure 3.4 below shows the INSTRON 8872 Universal Testing Machine that being used.

Figure 3.5 INSTRON 8872 Universal Testing Machine

3.4.1 Procedure of Tensile Testing

1. The thickness and width of the dog bone specimens were measured and the gauge length of 25mm was marked on the specimens.
2. The INSTRON 8872 Universal Testing Machine was started to function by switching on the plug. The setting to run the program for the tensile machine was done with the aid of technician.
3. In the computer software, the mechanical properties were selected among the wide range of choices before conducting the tensile test. Ultimate strength, yield strength, maximum displacement and Young's Modulus were chosen as the result that will be obtained.
4. The speed rate was set as 5mm/min.
5. After the setting the computer software, the tensile test specimens were clamped tightly aligned with the location set. The extensometer was then located at the gauge length that marked.
6. The tensile test was started by clicking the "start" indicator in computer and the tension is started to apply at one end and fixed at another end. Before starting the tensile test, "balance all" button was clicked.
7. Then, the extensometer was released when the strain was increased by 1%.
   Tension is continued to apply on the specimen.
8. Tensile test was done when the specimens were broke into two components.
9. Results were printed out and analyzed.

Figure 3.6 Tensile test specimen is gripped tightly

3.5 Compression Testing

Compression test is the test when the specimen experience opposing forces that push inward on the specimen from opposite sides. The specimen is located in between two plates that ready to sustain the distribution of applied force that across the entire surface area of two opposites faces of specimen and then one of the plates are pushed by a universal testing machine that cause the flattened of specimen. Basically, the specimen that being loaded will become shortened along with the applied forces direction and expands in the direction perpendicular to the force.

The main objective to conduct compression test is to find out the behaviour or response of a material by knowing its strain, stress and deformation. It is meant that all the parameter related to the mechanical properties of specimen can be determined such as compressive strength, yield strength, ultimate strength, elastic limit, and the elastic modulus.

Usually, after getting know the parameters and the values that associated with the specific material, it can been known whether the particular specimen is appropriate for the specific application or it will turn to failure under the specific stresses.

In this experimental work, compression test was done by using the Universal Testing Machine that known as model INSTRON 5585. The specimens were loaded between the platens of the machine until a certain load or extension has been reached. The data that taken was maximum load, area under curve, energy at maximum compressive stress. In details, it can be referred to APPENDIX C1, APPENDIX C2, APPENDIX C3 and APPENDIX C4.

3.5.1 Preparation of the Specimen for Experimental Work

The specimens for this study were circular shape and square shape. There were four different lengths which included 50mm, 100mm, 150mm and 200mm. To fabricate the tubes into these lengths, bandsaw machine had been used. After fabrication of tubes, 24 tubes which includes 12 circular tubes and 12 square tubes were sent to Agarwood supplier for the wood filling. Agarwood was decided to use as the wood for the experimental work. The filling of wood was done on the circular tube in Figure 3.7 and square tube in Figure 3.8

Figure 3.7 Wood filling of circular tube

Figure 3.8 Wood filling of square tube

3.5.1.1 Procedure

1. The tube was ensured to be secured in a tabletop vise and clamp prior to starting the cut as shown in Figure 3.9.

2. The blade of band saw was checked few times to make sure it is sharpened.

3. The band saw was set at the appropriate speed for the type of specimen.

4. Band saw was started to perform cutting when the On/Off starter button was pressed.

5. During cutting, water was squeezed onto the blade to reduce the friction of blade's surface and specimen's surface to prevent the blade from broken as shown in Figure 3.10.

6. On/Off starter was pressed to switch off the power when the cutting was done.

7. The specimen was removed once the saw came to a complete stop.

8. Lastly, the machine was left in a safe, clean and tidy state.

Figure 3.9 Preparation for cutting specimen

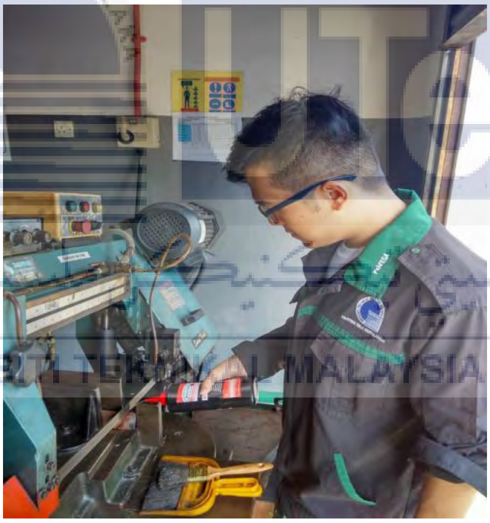

Figure 3.10 Water is put to reduce friction between blade and specimen surface

3.5.2 Conduct of Compression Testing

There were some steps of procedure that need to follow as shown below:

3.5.2.1 Procedure

1. UTM machine INSTRON 5585 in Figure 3.11 is made sure in a good condition before starting compression testing.
2. The computer software, Bluehill of UTM machine was initially setup by the aid from technician to make sure the compression test was ready to be started. The loading rate was set as 10mm/min.
3. The equipments that used such as Handycam Camcorder as shown Figure 3.12, LED lighting system, tripod stand as shown in Figure 3.13 were set up properly.
4. Dimensions of specimen was checked precisely to ensure the accuracy of the dimensions.
5. Ends of specimen was checked as the ends should be plane when located on the plate.
6. The specimen was placed centrally between the two compression plates to make sure the centre of moving head is just vertically above the centre of specimen.
7. Load was started to apply when clicked "start" button in computer meanwhile the camcorder was started to record simultaneously.
8. The load was applied on the specimen by moving vertically downwards the plates above specimen as shown in Figure 3.14.
9. Voice was recorded for every 5mm extension throughout the compression.
10. The loading force was stopped until the specimen fails or certain extension was reached.

11. Results that taken were being analysed as shown in Figure 3.15.

Figure 3.11 INSTRON Universal Testing Machines 5585

Figure 3.12 Sony Handycam Camcorder

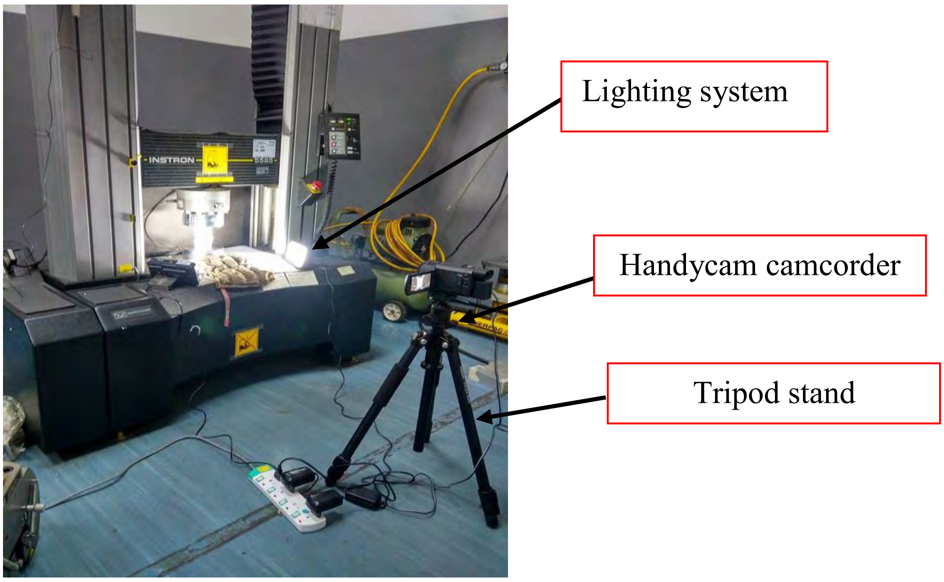

Figure 3.13 Setup of equipments for compression test

Figure 3.14 Conduct of compression test

Max Load [kN]	Compressive stress at Maximum Load [MPa]	Compressive strain (Extension) at Maximum Load [mm/mm]	Compressive extension at Maximum Load [mm]
> 61.9879	> 337.55	> 0.87	> 87.15

Area under curve [J]	Energy at Maximum Compressive stress [J]	Load at Yield (Offset 0.2 %) [kN]	Compressive stress at Yield (Offset 0.2 %) [MPa]
650.47	1126.72	-----	-----

Figure 3.15 Results of compression testing

3.6 Preparation of Final Report

A report on this study will be written at the end of the project and prepare for the final presentation.

CHAPTER 4

RESULT AND DISCUSSION

4.1 Introduction

This chapter describes the data and result that obtained from the tensile testing. The results get from the four testing specimens will be analyzed and compared in order to get an average reading of the mechanical properties such as ultimate strength, yield strength, maximum displacement and Young's Modulus.

4.2 Result of Tensile Test

There were four aluminum tensile test specimens being tested in order to get the average readings of the results. The Figure 4.1 below shows the tensile test specimens are broken into two pieces.

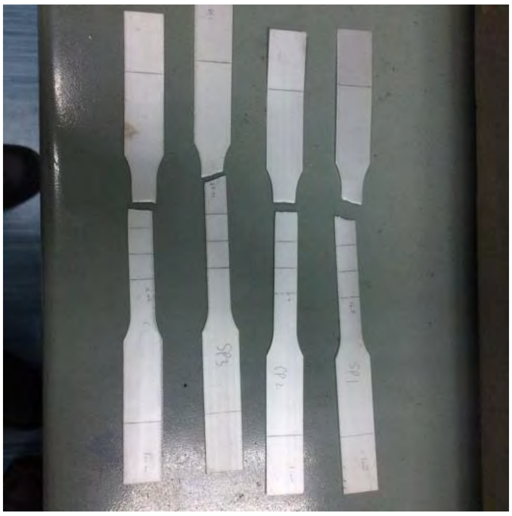

Figure 4.1 Tensile test specimens broken after testing

The results that came out from the tensile testing have shown many properties of the specimens such as maximum load, ultimate strength, load at yield strength, yield strength, load at break, tensile stress at break, tensile extension at break, tensile strain at break, strain at break and Young Modulus. The Figure 4.2 below shows the results of tensile test specimen 1.

Maximum Load [kN]	Tensile stress at Maximum Load [MPa]	Load at Yield (Offset 0.2 %) [kN]	Tensile stress at Yield (Offset 0.2 %) [MPa]
2.788	223.052	1.780	142.394

Load at Break (Standard) [kN]	Tensile stress at Break (Standard) [MPa]	Tensile extension at Break (Standard) [mm]
2.385	190.766	8.398

Tensile strain (Strain 1) at Break (Standard) [mm/mm]	Strain 1 at Break (Standard) [mm/mm]	Modulus (Automatic) [GPa]
0.336	0.010	1.567

Modulus (Automatic Young's) [GPa]	Modulus (E-modulus) [GPa]
73.293	50.665

Figure 4.2 Example results of tensile test specimen 1

Basically, there were four main mechanical properties that need to be determined which were ultimate strength, yield strength, maximum displacement and Young's Modulus. The results that obtained of the four specimens were then being analyzed and compared with the theoretical value of aluminum. Young Modulus's was being compared between them. The theoretical value of Young Modulus for aluminum is 69GPa. After comparing the results, it was found that the Young's Modulus of tensile test specimen 4 had the biggest difference with theoretical value. Thus, the result of tensile specimen 4 could be ignored.

The average value was taken from the other three tensile test specimens. The Table 4.1 below shows the results for ultimate strength, yield strength, maximum displacement and Young's Modulus of the three tensile test specimen.

Table 4.1 Result for the three tensile test specimens

Sample	Ultimate Strength (MPa)	Yield Strength (MPa)	Maximum Displacement (mm)	Young's Modulus (GPa)
1	223.052	142.394	8.398	73.293
2	199.863	126.969	6.301	72.942
3	202.609	130.294	8.250	68.200
Average	208.508	133.219	7.650	71.478

From the Table 4.1 above, it shows the average value for ultimate strengths, yield strength, maximum displacement and Young's Modulus. Therefore, it can be said that the experimental value for the aluminum after conducting tensile test is 208.508 MPa for ultimate strength, 133.219 MPa for yield strength, 7.650 mm for maximum displacement and 71.478 GPa for Young's Modulus.

The Figure 4.1, Figure 4.2 and Figure 4.3 show the graph of stress versus strain that produced from the tensile testing. The point 1 indicates the yield strength whereas the point 2 indicates the ultimate strength.

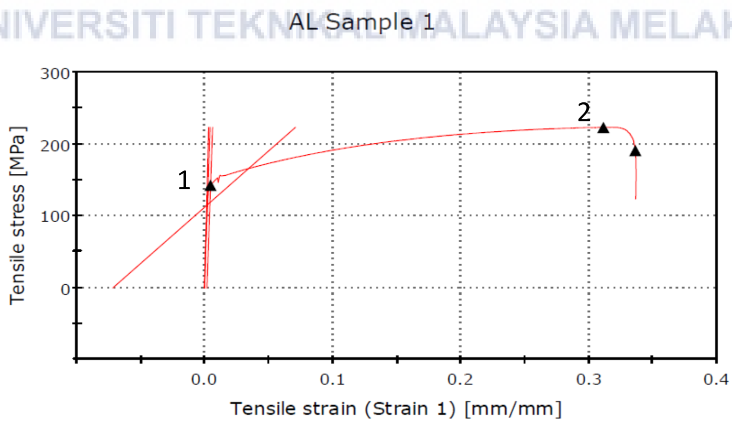

Figure 4.3 Tensile test specimen 1

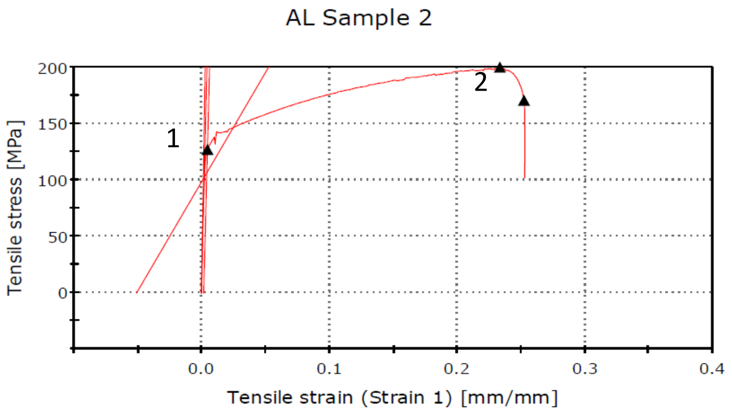

Figure 4.4 Tensile test specimen 2

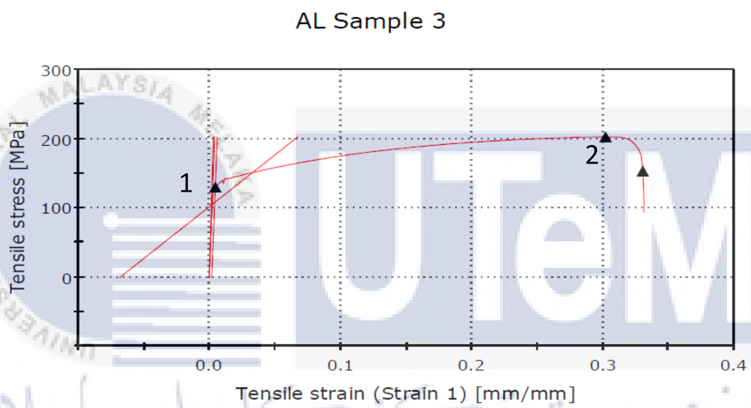

Figure 4.5 Tensile test specimen 3

4.3 Determination of Energy Absorption

Energy absorption of tube is calculated based on two methods. These two methods are used to calculate the useful energy which is the energy until the densification point.

4.3.1 First Method

In this study, one of the objectives is to find the energy absorption of tube. In order to study on how the presence of wood to enhance the energy absorption capacity of tube, the results need to be analysed properly through the load-displacement graph as shown in Figure 4.6.

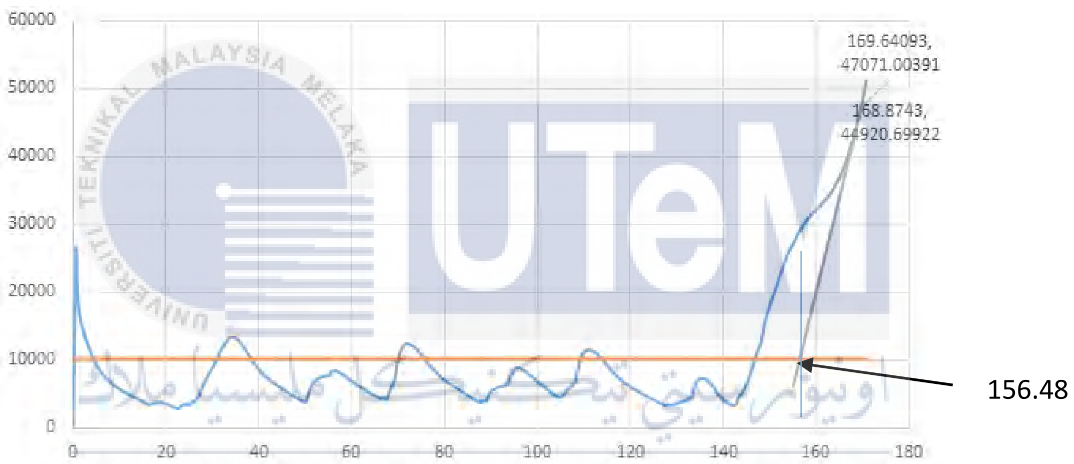

Figure 4.6 Load-displacement curve of square hollow tube 200mm

From the Figure 4.6, it can be found that there are three distinct regions in the graph which included linear elastic region, plateau region and densification region. In the linear elastic region, cell walls bending or stretching are controlling the deformation. This region is followed by a plastic collapse region which proceeded by spreading the local deformation and collapse to non-deformed region of the sample. This region is characterized by a load plateau with either a constant value or slight increase with displacement. In densification region, cell walls is considered densified when cell wall began to touch each other.

Through Figure 4.6, it is indicated that the mean load for the square tube can be determined by taking the average load from zero until the double of first peak load. Then a straight parallel line is plotted in order to find the intersection point with mean load which is known as densification point.

Thus, it is found that the displacement at densification point is 156.48mm. By knowing the densification point, the energy that calculated will be area under the graph before the densification point. This is because that particular area under the graph is known as useful energy. In this area, the compression is occurred on cellular of tube itself whereas the compression after the densification point is no longer compression on tube but between the metal of tubes.

4.3.2 Second Method

For another case, as shown in Figure 4.7, it is clearly seen that there are no double peak load in this graph.

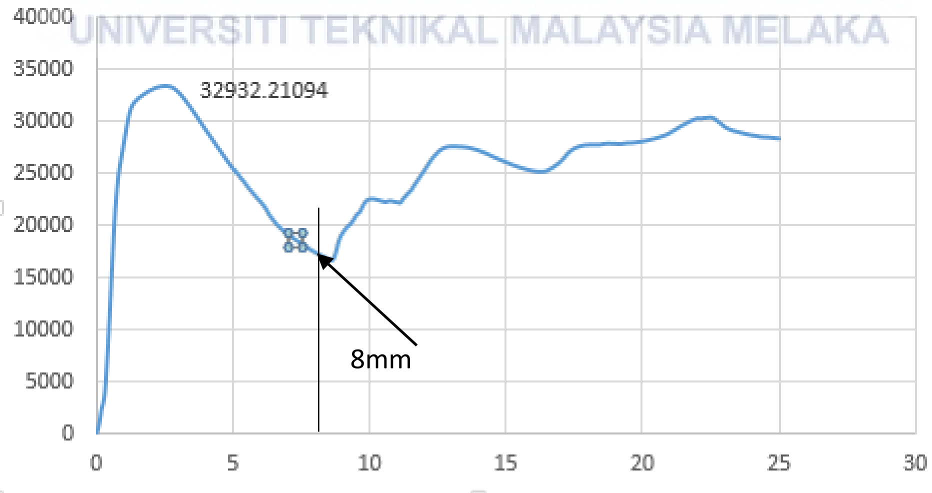

Figure 4.7 Load-displacement curve of 50mm wood-filled circular tube

Thus, in this case, the mean load and area under the graph are obtained based on the specific displacement that has been set. For example, 8mm of extension is set in this experiment. This indicates that the energy absorption is determined by knowing the area under the graph until 8mm displacement.

4.4 Analysis of Quasi-Static Test

In order to analyse the results get from quasi-static test, firstly it is necessary to know how to see the graph according to the compressed tube. The deformation mode need to be determined in order to calculate the energy absorption, mean load and plastic wavelength. So, the analysis of results will be done through the load-displacement graph as shown in Figure 4.8.

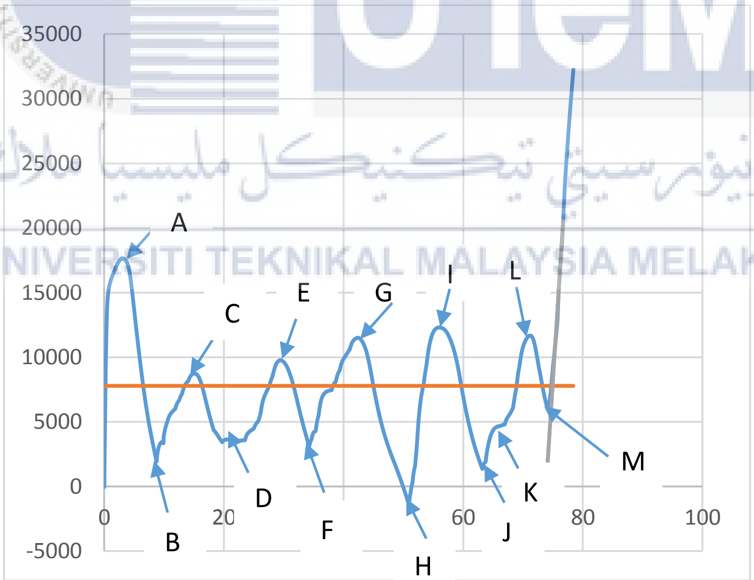

Figure 4.8 Load-displacement curve of 100mm tube

From Figure 4.8, it is clearly seen the deforming mode is in the axisymmetric mode. This can be known through the behaviour of the graph. The graph shows the presence of linear elastic region, plateau region and densification region. Alternate high and low peak loads characterize this curve. These peaks indicates the deformation of the outward and inward parts of the folds. Prior to buckling, an axisymmetric deformation mode buckles is observed near the top or bottom ends of the specimens.

Video is recorded during the compression test and the sequence of configurations illustrating progressive crushing of a tube will be shown in Figure 4.9. According to Figure 4.9, the platens of machine cause the usual boundary layer lobes to start form at the end of the tubes. The equilibrium curve reaches the maximum load level at point A which is 4mm without changing the mode of tube. At this point, the wall starts to bend outward and the force drops sharply until the first fold completely formed as the loading is continued. The forces reaches its minimum B which is 10mm, and begin to increase again. The wall near the deformed zone tends to bend inward and another force peak C which is 16mm appears at the moment of appearance of internal buckling pattern. The force then decreases as the wall bends inwards. After a small bending of the wall at D which is 20mm, the force begins to increase again until point E which is 30mm, and one lobe is formed. The pattern is repeated until 75mm displacement which is point M. It is deformed with three lobes lastly.

In details for the deformation of circular and square tube, it can be referred to APPENDIX B1, APPENDIX B2, APPENDIX B3 and APPENDIX B4.

Point A (δ=4mm)

Point B (δ=10mm)

Point C (δ =16mm)

Point D (δ=20mm)

Point E (δ=24mm)

Point F (δ=34mm)

Point G (δ=43mm)

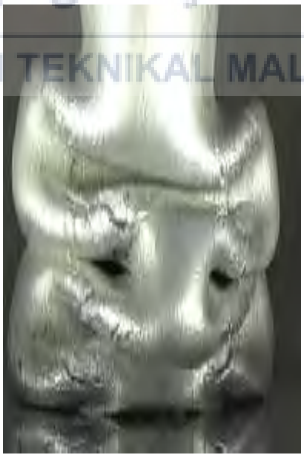

Point H (δ=50mm)

Point I (δ=55mm)

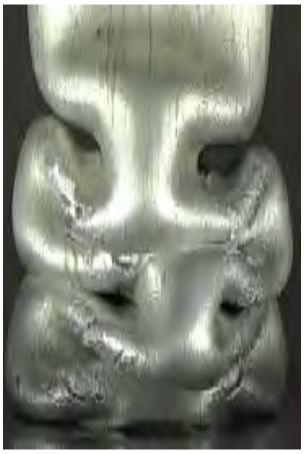

Point J (δ=63mm)

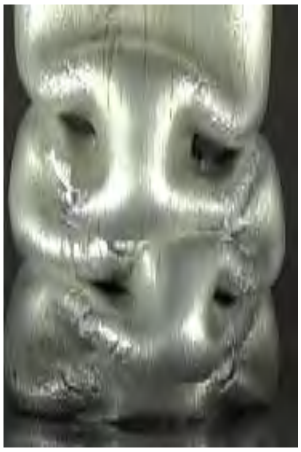

Point K (δ=63mm)

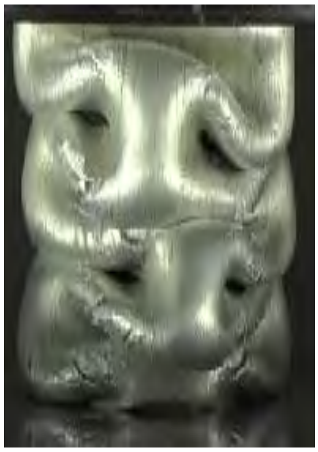

Point L (δ=72mm)

Point M (δ=75mm)

Figure 4.9 Sequence of configurations illustrating progressive crushing of a tube

4.5 Axial Crushing of Circular Hollow Tube

Experimental value for peak load, mean load, plastic half fold length, energy and specific energy is shown in Table 4.2.

Table 4.2 Experimental value for peak load, mean load, plastic half fold length, energy and specific energy

Specimen	Peak Load (N)	Mean Load at densification (N)	H (mm)	Energy (J)	Specific Energy (kJ/kg)	Note
50mm	24435.6	18939.2	5.4	146.622	60.3	Local Buckling
100mm	14647.85	7783.874	12	103.131	43.1	Local Buckling
150mm	-	-	-	-		Global Buckling
200mm	-	-	-	-		Global Buckling

Table 4.3 Comparison between experimental value and theoretical value for mean load

Specimen	Experimental Mean Load (N)	Theoretical Mean Load (N)	Percentage Difference (%)
50mm	18939.2	14617.29	29.5
100mm	7783.874	7146.437	8.9

Table 4.4 Comparison between experimental value and theoretical value for plastic wavelength

Specimen	Experimental Plastic Wavelength, 2H (mm)	Theoretical Plastic Wavelength, 2H (mm	Percentage Difference (%)
50mm	10.8	11.7	7.8
100mm	15	11.7	28.2

Figure 4.10 Compressed circular hollow tube

From Figure 4.10, it can be seen the 50mm circular hollow tube exhibit a progressive axisymmetric deformation mode. There are four lobes of deformation after the crushing of the tube.

The first lobe is formed started at the uppermost section. Each peak in the load-displacement curves shown is associated with the formation of one lobe. The first peak load is 24.435KN. The corresponding values for the other peak is smaller than the value of the first peak. This is because the specimen is free of all distortions when the formation of the first peak. So, the formation of the next fold is influenced by the deformations that formed during first fold by inducing a local bending at the plastic hinges level. Thus, it is noticeable that the corresponding peak value is lower than the first peak.

From Table 4.2, it can be seen the 50mm tube has the best performance because energy and specific energy is the highest which is 146.622J and 60.3kJ/kg respectively. Besides, from

Table 4.3, there is 29.5% percentage difference for mean load while 7.8% percentage difference for plastic wavelength can be known from Table 4.4.

Figure 4.11 Compressed circular hollow tube

From Figure 4.11, 100mm tube developed three axisymmetric folds. From Table 4.2, it is found that the energy absorbed by 100mm tube is 101.131J and 43.1kJ/kg for the specific energy. Thus, it means that the energy absorbed by the 100mm tube which collapsed with mixed mode is lesser than the 50mm with concertina mode. This is because mixed mode that happened on the tube may induces asymmetry which may lead to global bending mode which is Euler-type buckling failure, which is extremely limit the capacity of energy absorption. Hence, it is more desirable to use the structure that deformed with axisymmetric mode since it promises a progressive collapse. From Table 4.3, there is 8.9% percentage difference for mean load while 28.2% percentage difference for plastic wavelength can be seen from Table 4.4.

For 150mm and 200mm tubes, they are deformed with global buckling mode as shown in Figure 4.12 and Figure 4.13. This indicates that long tubes lead to inefficiency of energy absorption.

The four different length of circular tubes have the same diameter and thickness which is 25.3mm and 1.5mm respectively. This indicates that the 50mm tube has 16.84 of D/h and

1.97 of L/h. It is observed that 50mm tube is collapsed with concertina mode. For the 100mm tube, its D/h is 16.87 and L/h is 3.95. It is observed that 100 tube is collapsed with mixed mode.

By referring to Figure 4.14, for D/h less than 50, concertina mode is present for L/h less than 2 and mixed mode for L//h larger than 2. So it is theoretically proven.

Figure 4.12 Global buckling failure of 150mm tube

Figure 4.13 Global buckling failure of 200mm tube

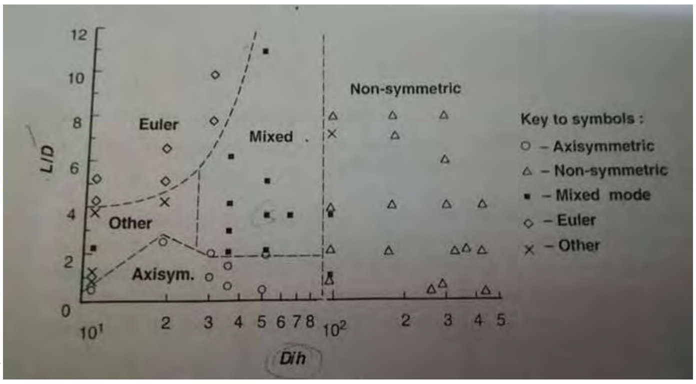

Figure 4.14 Mode of classification for circular aluminium tube (Guillow et.al., 2001)

4.6 Axial Compression of Wood-Filled Circular Tube

To obtain a highly efficient energy absorption component, the aluminium tube can be filled with solid wood in order to improve the crashworthiness. This is due to the good interaction between solid wood and tubes that gives an extra improvement in energy dissipation. Solid wood just like a constraint to restrict the tube wall when it wants to buckle inwardly. However, the solid wood is able to bend freely outward without any constraint from wood. This constraint of wood will bring two effects. First, the solid wood may change the deformation mode of the tube depending upon the plateau stress: for circular tube, from the diamond mode of an empty tube to the ring mode, and for square tubes, from non-compact mode to compact mode. Second, even if the collapse mode seems to be the same, the energy absorption capacity can be enhanced by the presence of the wood.

When wood are compressed, densification occurs after the plateau stage and the stress increases rapidly with the strain. The corresponding strain, the locking strain, is the limit of the compression stroke achievable by the tube and this leading to a higher average force.

Table 4.5 Experimental value for peak load, mean load, plastic half fold length, energy and specific energy

Length of Specimen	Specimen	Peak Load (N)	Mean load at ʃ =8mm (N)	Theoretical Mean Load (N)	Energy (J)	Specific Energy (kJ/kg)	Note
50mm	Sample 1	27669.59	18125.93	24828.9	189.9331	45.36	Local Buckling
	Sample 2	33386.85	17502.49	24828.9	198.7678	47.47	Local Buckling
	Sample 3	33239.56	24502.62	24828.9	198.8392	47.49	Local Buckling
	Average	**31432.00**	**20043.68**	**24828.9**	**195.8467**	**46.77**	
100mm	Sample 1	31974.42	22183.22	17994.61	197.1631	45.64	Local Buckling
	Sample 2	30000.65	20570.88	17994.61	175.8563	40.71	Local Buckling
	Sample 3	33009.14	26101.86	17994.61	211.2472	48.90	Local Buckling
	Average	**31661.40**	**22952.00**	**17994.61**	**194.7555**	**45.08**	
150mm	Sample 1,2,3	-	-	-	-	-	Global buckling
200mm	Sample 1,2,3	-	-	-	-	-	Global buckling

Table 4.6 Comparison between experimental value and theoretical value for mean load

Specimen	Experimental Mean load	Theoretical Mean Load	Percentage Difference (%)
50mm	20043.68	24828.90	19.30
100mm	22952.00	17994.61	27.55

Based on the Figure 4.15 and Figure 4.16, it can be seen that the 50mm tube is collapsed with concertina mode while 100mm tube is collapsed with diamond mode. For both 150mm and 200mm tubes, they resulted with global buckling which shown by Figure 4.17 and Figure 4.18.

The energy absorption of circular tube filled with solid wood for 50mm is 195.8467J and 194.7555J for 100mm. For specific energy, 46.77kJ/kg for 50mm tube and 45.08kJ/kg for 100mm tube. Thus, the 50mm tube shows a slightly better performance in energy absorption and specific energy absorption than 100mm tube. For the long tube 150mm and 200mm, Euler-type buckling takes place.

From Table 4.5, it is clearly seen that the mean load of 50mm tube which is 24828.9N is higher than 100mm tube which is 17994.61N. For the percentage difference between theoretical value and experimental value, 50mm tube has 19.3% whereas 100mm tube has 27.55 % as presented in Table 4.6.

Figure 4.15 Deformed mode of 50mm wood-filled tube

Figure 4.16 Deformed mode of 100mm wood-filled tube

Figure 4.17 Deformed mode of 150mm wood-filled tube

Figure 4.18 Deformed mode of 200mm wood-filled tube

4.6.1 Comparison of Circular Hollow Tube and Wood-Filled Tube

Table 4.7 Comparison of energy absorption and specific energy absorption of hollow tube and wood-filled tube

Length of Specimen (mm)	Energy of hollow tube (J)	Energy of wood filled tube (J)	Specific Energy of hollow tube (kJ/kg)	Specific Energy of wood filled tube (kJ/kg)
50	146.622	195.8467	60.3	46.77
100	103.131	194.7555	43.1	45.08
150	-	-	-	-
200	-	-	-	-

From the Table 4.7, it can be clearly seen that for the energy absorption, 50mm wood-filled tube shows the best energy absorption which is 195.8467J. It is found that even if the collapse mode appear the same, the energy absorption capacity can be enhanced by the presence of the wood. Next, for the specific energy absorption, the 50mm hollow tube shows the best specific absorption which is 60.3kJ/kg.

4.7 Axial Crushing of Square Hollow Tube

Figure 4.19 Deformed mode of 200mm square hollow tube

Based on Figure 4.19, it can be seen that the tube wall goes through intense inward and outward plastic bending with possible stretching. The contiguous fold that formed during the progressive buckling from one end of specimen is known as compact mode. When the tube is thin, it may occur a non-compact collapse. In this case, the folds are not continuous, and separated by a distance approximately equal to the side length of tube

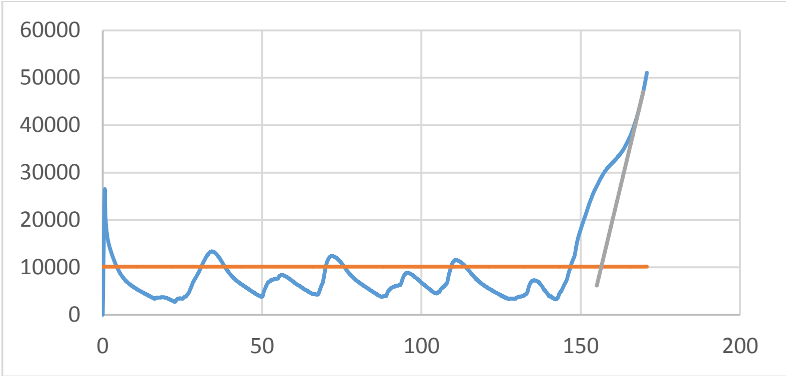

Figure 4.20 Load-displacement curve of 200mm square hollow tube

From Figure 4.20, it is clear that the force falls sharply after the initial peak and then it fluctuates periodically, corresponding to the formation and complete collapse folds one by one. There are two modes of deformation which are compact mode and non-compact mode. From Figure 4.19, it is found that the tube is deformed in compact mode which in diamond mode.

Table 4.8 Experimental value for peak load, mean load, plastic half fold length, energy and specific energy

Specimen (Sample 1)	**Peak Load (N)**	**Mean Load at densification (N)**	**H (mm)**	**Energy (J)**	**Specific Energy (kJ/kg)**	**Note**
50	27157.84	9887.6	15	100.622	21.76	Local Buckling
100	29725.60	12692.35	17	111.727	24.37	Local Buckling
150	27675.78	10284.4	18	96.146	20.86	Local Buckling
200	26520.93	10161.48	15	92.391	20.12	Local Buckling

Table 4.9 Comparison between experimental value and theoretical value for mean load

Sample 1	Experimental Mean Load (N)	Theoretical Mean Load (N)	Percentage Difference (%)
50mm	9887.6	11661	15.2
100mm	12692.35	11661	8.8
150mm	10284.4	11661	11.8
200mm	10161.48	11661	12.8

Table 4.10 Comparison between experimental value and theoretical value for plastic wavelength

Sample 1	Experimental Plastic Wavelength, 2H (mm)	Plastic Wavelength, 2H (mm)	Percentage Difference (%)
50mm	30	27.4	9.5
100mm	34	27.4	24.1
150mm	36	27.4	31.38
200mm	30	27.4	9.5

From the Table 4.8, it can be found that all the tubes with different length deformed with local buckling which is diamond mode. Among the four tubes, 100mm tube has the best energy absorption and specific energy absorption which is 111.727J and 24.37kJ/kg respectively.

From Table 4.9, it can be seen that the highest percentage difference of mean load is 50mm which is 15.2% while the highest percentage difference for plastic wavelength is 150mm which is 31.38% from Table 4.10.

4.8 Axial Compression of Wood-Filled Square Tube

Table 4.11 Experimental value for peak load, mean load, plastic half fold length and energy

Length of Specimen	Specimen	Peak Load (N)	Mean load at ʃ =8mm (N)	Theoretical Mean Load (N)	Energy (J)	Specific Energy (kJ/kg)	Note
50mm	Sample 1	61388.78	34486.21	49117.22	306.2864	27.35	Local Buckling
	Sample 2	55895.17	34203.03	49117.22	306.8587	26.45	Local Buckling
	Sample 3	45959.11	31605.69	49117.22	232.3160	20.74	Local Buckling
	Average	**54414.35**	**33431.64**	**49117.22**	**281.8204**	**24.85**	Local Buckling
100mm	Sample 1	53236.08	35152.17	49117.22	291.1561	25.1	Local Buckling
	Sample 2	51487.44	34881.86	49117.22	306.2629	26.4	Local Buckling
	Sample 3	47355.65	31203.04	49117.22	269.3393	23.2	Local Buckling
	Average	**50693.06**	**33745.69**	**49117.22**	**288.9194**	**24.9**	Local Buckling
150mm	Sample 1	42387.9	33402.75	49117.22	250.390	20.2	Local Buckling
	Sample 2	54893.01	35124.45	49117.22	314.1648	29.3	Local Buckling
	Sample 3	47225.51	31734.46	49117.22	258.6936	20.9	Local Buckling
	Average	**48168.81**	**33420.55**	**49117.22**	**274.4163**	**23.5**	Local Buckling
200mm	Sample 1	49410.67	31860.45	49117.22	248.7099	19.6	Local Buckling
	Sample 2	54419.03	36757.70	49117.22	296.1053	23.3	Local Buckling
	Sample 3	46446.13	37793.11	49117.22	283.7590	22.3	Local Buckling
	Average	**50091.94**	**35470.42**	**49117.22**	**276.1914**	**21.7**	Local Buckling

Table 4.12 Comparison between experimental value and theoretical value for mean load

Specimen	Experimental Mean load	Theoretical Mean Load	Percentage Difference (%)
50mm	33431.64	49117.22	32.5
100mm	33745.69	49117.22	31.3
150mm	33420.55	49117.22	32
200mm	35470.42	49117.22	27.8

Based on Figure 4.21, Figure 4.22, Figure 4.23 and Figure 4.24, it is clearly seen that all the tubes with 50mm, 100mm, 150mm and 200mm are deformed with local buckling which is diamond mode. Although the tube are split, but before it breaks, it already undergo the diamond mode of deformation. So, the energy that determined is useful energy which is the area under the curve before it breaks.

From Table 4.11, it can be found that the 100mm tube has the best energy absorption which is 288.9194J then followed by 50mm, 200mm and 150mm. Same goes to the specific energy absorption, 100mm tube has the best performance which is 24.9kJ/kg followed by 50mm, 150mm and 200mm. Through Table 4.12, it is clearly seen that, the 200mm has the lowest percentage difference of mean load between theoretical value and experimental value which is 27.8%.

Figure 4.21 Deformed mode of 50mm wood-filled tube

Figure 4.22 Deformed mode of 100mm wood-filled tube

Figure 4.23 Deformed mode of 150mm wood-filled tube

Figure 4.24 Deformed mode of 200mm filled wood-filled tube

4.8.1 Comparison of Square Hollow Tube and Wood-Filled Tube

Table 4.13 Comparison of energy of hollow tube and wood filled tube

Length of Specimen (mm)	Energy of hollow tube (J)	Energy of wood-filled tube (J)	Specific Energy of hollow tube (kJ/kg)	Specific Energy of wood-filled tube (kJ/kg)
50	100.622	281.8204	21.76	24.85
100	111.727	288.9194	24.37	24.90
150	96.146	274.4163	20.86	23.50
200	93.391	276.1914	20.12	21.70

From Table 4.13, it can be found that for the energy absorption, 100mm wood-filled tube shows the best energy absorption and specific energy absorption which is 288.9194J and 24.90kJ/kg respectively.

4.9 Comparison of Square Tube and Circular Tube

Table 4.14 Comparison of energy and specific energy of circular tube and square tube

	Length of Specimen (mm)	Energy of hollow tube (J)	Energy of wood filled tube (J)	Specific Energy of hollow tube (kJ/kg)	Specific Energy of wood filled tube (kJ/kg)
Circular tube	50	146.622	195.8467	60.3	46.77
	100	103.131	194.7555	43.1	45.08
	150	-	-	-	-
	200	-	-	-	-
Square tube	50	100.622	281.8204	21.76	24.85
	100	111.727	288.9194	24.37	24.90
	150	96.146	274.4163	20.86	23.50
	200	93.391	276.1914	20.12	21.70

Based on the Table 4.14, it is clearly seen that square tube filled with wood has the best energy absorption when comparing to the same length of 50mm, 100mm, 150mm and 200mm. For 50mm, the energy absorption is 281.8204J, 288.9194J for 100mm, 274.1914J for 150mm and 276.1914J for 200mm.

For specific energy absorption, 50mm circular hollow tube has the highest absorption which is 60.3kJ/kg. For 100mm tube, circular tube filled with wood has the highest specific energy absorption which is 45.08kJ/kg. For 150mm tube, square tube filled with wood has the highest specific energy absorption which is 23.50kJ/kg. For 200mm tube, square tube filled with wood has the highest specific energy absorption which is 21.70kJ/kg.

It indicates that the presence of wood enhances the energy absorption of tube through the interaction of wood with tube when crushing is happened.

4.10 Energy Absorption

Best results of energy absorption for each length are determined and superimposed in a graph as shown in Figure 4.23.

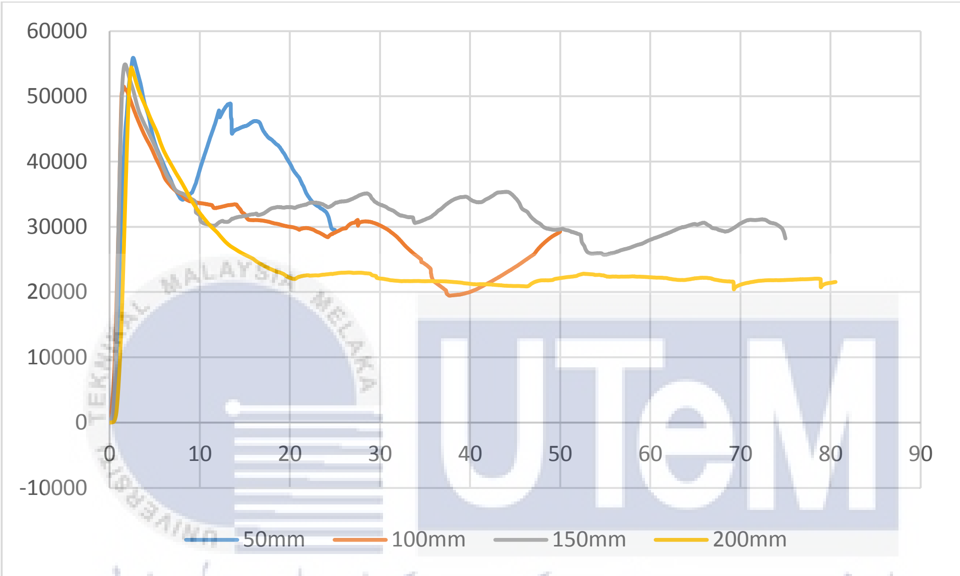

Figure 4.25 Superimposed graph of best result for each length of tube

Table 4.15 Highest energy absorption of tubes

Length (mm)	**Specimen**	**Energy absorption capacity (J)**
50	Wood-filled square tube	281.8204
100	Wood-filled square tube	288.9194
150	Wood-filled square tube	274.4163
200	Wood-filled square tube	276.1914

As for the energy absorber that is in the static condition, such as road safety barrier, it does not concern about the weight of the structure. It does not matter on how light or how heavy the structures are, and most importantly it manage to exhibit a higher energy absorption capacity.

The highest energy absorption of specimens are presented in Table 4.15. For such energy absorber, 100mm wood-filled square tube is the best choice because it has the highest energy absorption capacity which is 288.9194J.

4.11 Specific Energy Absorption

The specific energy absorption capacity are presented in Table 4.16. Specific energy absorption is a measure of energy absorption of a structural element. Thus, it is very important as it will be considered in the design of impact energy absorber in the application in aerospace, automotive and ground transportation.

Table 4.16 Specific energy absorption of specimen

Length (mm)	Specimen	Specific energy absorption capacity (kJ/kg)	Energy Absorption capacity (J)
50	Circular hollow tube	66.30	146.6220
100	Wood-filled circular tube	45.08	194.7555
150	Wood-filled square tube	23.50	274.4163
200	Wood-filled square tube	21.70	276.1914

As a common impact energy absorbers, thin-walled structures such as aluminum tube is broadly used in the crashworthiness application such as automotive industry to prevent injuries to the occupants when there is collision happened.

The reason why thin-walled structures often used as energy absorber is because of their high energy absorption capacity, economic price and weight efficient. Therefore, the specific energy absorption which is energy absorption per unit mass is the most greatly adopted index to evaluate the efficiency of energy devices.

The performance of the energy absorber can be known through the value of specific energy absorption. The higher the specific energy absorption, the more efficient the energy absorber. A good energy absorber must not only achieve a lightweight design, it also has to show high-quality capacity of energy absorption with the satisfactorily weight efficiency. This is because a high quality energy absorber due to the lightweight itself, so the specific energy absorption can become higher which is for impact energy devices.

From Table 4.16, it is noticeable that 50mm circular hollow tube has the lowest energy absorption capacity which is 146.622J, but it has the highest specific absorption which is 66.30kJ/kg. This indicates that 50mm circular hollow tube is the lightest since specific energy is energy per unit mass.

Thus, it is the best choice to be the structure in the application of energy absorber device due to its light weight and high specific energy absorption capacity. Light weight of structures able to reduce the fuel consumption. This directly means that the automobiles can travel with high speed due to its light weight but this will lead to a higher probability to cause the occupants sustain the critical impact. So, specific energy absorption plays an important roles in designing a structures such as aerospace and automobile to get a good structure with balance of weight efficiency and fuel consumption to secure the occupants in the transportations.

4.12 Comments on the Results

In overall, the percentage difference between theoretical value and experimental value for mean load and plastic wavelength is about 30%. So, it is still within the acceptable range. For the mean load, square tubes show a higher value of mean load then circular tubes. This indicates that square tube able to absorb more energy since the energy determined through the area under the curve of load-displacement graph. For the plastic wavelength, circular hollow tube a shorter plastic wavelength absorb more energy than square hollow tube. So, it can be said that the lower plastic wavelength the higher the energy absorption.

The deviation of the theoretical value with experimental value may be affected by the geometry imperfection of the tubes. Human error must be taken into account as the tubes are manually fabricated. It is also found that angle at the edge of the tube is slightly inaccurate as what as expected. This may due to the rusty and blunt of blade of bandsaw machine used to fabricate the tubes without replacement. Moreover, the filling wood into the tube by the supplier is imperfect. The wood is not fully contact with the tube so some part of the tube cannot produce a perfect folding formation. Unflat surface of tube may cause the contribution to the deviation too. This is because global buckling might happen during the experiment when the surface of tube is uneven and not completely flat. The specimen is considered failed if deformed with global buckling.

Thus, there are some methods to reduce the deviations. One of the methods is improving the geometry imperfection by fabricating the tube as precise as possible. The eyes contact must be perpendicular to the line that drawn on the tube to make sure blade is aligned with the line. To improving the surface flatness, the grinding process has to be done properly. A straight line can be drawn on the tube to be a guideline when grinding. The wood dimension have to be measured precisely to make sure it is fit enough for putting into the tube and fully touching the inner surface of tube.

4.13 Theoretical Calculation for Mean Load and Plastic Half Fold Length

According to the Abramowicz and Jones (1984), for the circular hollow tube which deformed with concertina mode, the mean load is determined by using the formula as shown below:

$\text{Yield strength}, Y = 208.508MPa$

$Diameter, D = 25.3mm$

$Thickness, h = 1.5mm$

$$P_m = 8.91Yh\sqrt{Dh}\left(1 - 0.61\sqrt{\frac{h}{D}}\right)$$

$$P_m = 8.91(208.508 \times 10^6 \times 0.0015 \times \sqrt{(0.0015)(0.0253)}\left(1 - 0.61\sqrt{\frac{0.0015}{0.0253}}\right)$$

$$P_m = 14617.29N$$

According to the theoretical studies conducted by Singace (1999), for the circular hollow tube which deformed with non-symmetric modes, the mean load is determined by using the formula as shown below:

$Number\ of\ circumferential\ lobes, n = 3$

$Fully\ plastic\ bending\ moment\ per\ unit\ length, M_o = \frac{\sigma t^2}{4}$

$Diameter, D = 25.3mm$

$Thickness, h = 1.5mm$

$$M_0 = \frac{208.508 \times 10^6 (0.0015)^2}{4} = 117.3$$

$$\frac{P_m}{M_o} = -\frac{\pi}{3}\text{n} + \frac{2\pi^2}{n}\tan\left(\frac{\pi}{2n}\right)\frac{D}{\text{h}}$$

$$\frac{P_m}{117.3} = -\frac{\pi}{3}(3) + \frac{2\pi^2}{3}\tan\left(\frac{\pi}{2(3)}\right)\frac{0.0253}{0.0015} = 7146.437\text{N}$$

For the circular tube filled with wood which deformed with concertina mode, the mean load is determined by using the formula as shown below:

For sample tube 50mm,

$\boldsymbol{P_m = (P_m)_{tube} + (P_m)_{wood}}$

$Yield\ stength, \sigma_Y = 20.3125MPa$

$Area\ of\ contact, A = 5.0273 \times 10^{-4} m^2$

$$(P_m)_{wood} = \sigma_Y \times A$$

$$(P_m)_{wood} = \frac{130000}{0.08 \times 0.08} \times \frac{\pi(0.0223)^2}{4}$$

$$(P_m)_{wood} = (20.3125 \times 10^6) \times 5.0273 \times 10^{-4}$$

$$10211.6N$$

$$P_m = 14617.29N + 10211.6N = 24828.9N$$

For the square hollow tube which deformed with diamond mode, the mean load is determined by using the formula as shown below:

$Thickness, h = 1.35mm$

$side\ length, c = 44.65mm$

$$P_m = 9.56Yh^{\frac{5}{3}}c^{\frac{1}{3}}$$

$$P_m = 9.56Y(0.00135)^{\frac{5}{3}}(0.04465)^{\frac{1}{3}} = 11661N$$

For the square tube filled with wood which deformed with diamond mode, the mean load is determined by using the formula as shown below:

For sample tube 50mm,

$Yield\ stength, \sigma_Y = 20.3125MPa$

$Area\ of\ contact, A = 5.0273 \times 10^{-4} m^2$

$$P_m = (P_m)_{tube} + (P_m)_{wood}$$

$$(P_m)_{wood} = \sigma_Y \times A$$

$$(P_m)_{wood} = \frac{130000}{0.08 \times 0.08} \times 0.04195^2$$

$$(P_m)_{wood} = (20.3125 \times 10^6) \times 1.76 \times 10^{-3} = 37456N$$

$$P_m = 11161N + 37456N = 48617N$$

For the half-length of fold, H for square hollow tube,

$Ultimate\ strength, Y = 208.508MPa$

$Thickness, h = 1.35mm$

$side\ length, c = 44.65mm$

$$H = 0.983^3\sqrt{hc^2}$$

$$H = 0.983\sqrt[3]{0.00135 \times 0.04465^2} = 13.68mm$$

For the half-length of fold, H for circular hollow tube,

$Diameter, D = 25.3mm$

$Thickness, h = 1.5mm$

$$H = 0.95\sqrt{Dh} = 0.95\sqrt{0.0253 \times 0.0015} = 5.85mm$$

CHAPTER 5

CONCLUSION & RECOMMENDATIONS FOR FUTURE RESEARCH

5.1 Conclusion

The quasi-static crushing behaviour of hollow tube and wood-filled tube are investigated experimentally and theoretically. The experimental value is agree reasonably with the theoretical value. Circular hollow tubes collapse with axisymmetric mode which is concertina mode and mixed mode, and Euler-failure mechanism for the long tubes when axially crushed. Besides, square hollow tubes and square wood-filled tube collapse with compact mode which is diamond mode. With the presence of solid wood, overall energy absorption capacity performance of tube is enhanced. In this experimental work, it is found that 50mm circular hollow tube with 66.30kJ/kg specific energy absorption is the best structure for the application in aerospace and automobile as a energy absorber due to the high specific energy absorption and light weight. For the static energy absorber like road safety barrier, 100mm wood-filled square tube is the best choice because it has the highest energy absorption capacity which is 288.9194J. It indicates that the higher mean load brings the higher energy absorption capacity. Plastic wavelength of circular hollow tube is found lesser than square tube since circular hollow tube has higher energy absorption compared with square hollow tube. There are some factors that contribute to the difference of theoretical value and experimental value such as imperfection of the tube geometry and the surface flatness of the tube. In order to improve the result, the tube geometry must be fabricated as precise as possible.

5.2 Recommendations for Future Research

In this study, it is shown that the wood-filled tube exhibits the highest energy absorption while hollow tube exhibits the highest specific energy absorption. There are some recommendations for the next study that will be conducted. It is recommended that the "Agarwood" can be compared with the other types of wood in term of the energy absorption capacity. There are some local wood that manage to be found in Malaysia such as "Rambutan wood", "Durian wood", "Akasia wood" and so forth. The energy absorption and weight of wood can be compared and find out the highest specific energy absorption with the lightest weight. For the length of tubes, it is suggested to use a shorter various length of tubes such as 50mm, 75mm and 100mm. In this range of lengths, the tubes are either collapse in axisymmetric mode or non-symmetric mode. The longer tubes which are 150mm and 200mm shows a lower performance of energy absorption and easily lead to global buckling which is Euler-failure mechanism. The specimen is considered failed once deformed with global buckling.

REFERENCES

Abramowicz, W. (1983). The effective crushing distance in axially compressed thin-walled metal columns. *International Journal of Impact Engineering*, *1*(3), 309-317.

Abramowicz, W. (2003). Thin-walled structures as impact energy absorbers. Thin-Walled Structures, 41(2–3), 91–107.

Abramowicz, W., & Jones, N. (1984). Dynamic axial crushing of square tubes. International Journal of Impact Engineering, 2(2), 179-208.

Abramowicz, W., & Jones, N. (1986). Dynamic progressive buckling of circular and square tubes. Int. J. Impact Engng.4, 243-70.

Alavi Nia, A., & Parsapour, M. (2014). Comparative analysis of energy absorption capacity of simple and multi-cell thin-walled tubes with triangular, square, hexagonal and octagonal sections. Thin Walled Structures, 74, 155–165.

Alexander, JM. (1960) An approximate analysis of the collapse of thin cylindrical shells under axial load. Quart. J. Mech. App. Math. 13, 10-15.

Alghamdi, A. A. A. (2001). Collapsible impact energy absorbers: An overview. Thin-Walled Structures, 39(2), 189–213.

Aljawi, A. A. N. (2002). Numerical simulation of axial crushing of circular tubes. *JKAU: Eng. Sci*, *14*(2), 3-17.

Andrews, K. R. F., England, G. L., & Ghani, E. (1983). Classification of the axial collapse of cylindrical tubes under quasi-static loading. International Journal of Mechanical Sciences, 25(9-10), 687-696.

ASTM, E8. (2001). Standard test methods for tension testing of metallic materials. Annual book of ASTM standards. ASTM.

Beer, F. P., Johnston, R., Dewolf, J., & Mazurek, D. (2009). Mechanics of Materials, McGraw-Hill.

Bucur, V. (2006). Acoustics of wood. Springer Science & Business Media.

Davis, J. R. (Ed.). (2004). Tensile testing. ASM international.

DiPaolo, B. P., & Tom, J. G. (2006). A study on an axial crush configuration response of thin-wall, steel box components: The quasi-static experiments. International journal of solids and structures, 43(25), 7752-7775.

Duarte, I., Vesenjak, M., Krstulović-Opara, L., Anžel, I., & Ferreira, J. M. F. (2015). Manufacturing and bending behaviour of in situ foam-filled aluminium alloy tubes. Materials and Design, 66(PB), 532–544.

Florence, A. L., Gefken, P. R., & Kirkpatrick, S. W. (1991) Dynamic plastic buckling of copper cylindrical shells. International Journal of Solids and Structures, 27(1), 89–103.

Guillow, S.R., Lu, G. abd Grzebieta, R.H. (2001) Quasi-static axial compression of thin-walled circular aluminium tubes. Int. J. Mech. Sci. 43, 2103-23.

Johnson, W. (1990) Impact Strength of Materials. Edward Arnold, London.

Johnson, W., Soden, P.D and Al-Hassani. S.T.S (1977b) Inextensional collapse of thin-walled tubes under axial compression. J. Strain Analysis 12, 317-30.

Jones, N. (2012). Structural impact. PhD Proposal, 1, 425–478. [online] Available at: https://doi.org/10.1017/CBO9781107415324.004 [Accessed on 4 December 2016].

Karman, T. V. (1941). The buckling of thin cylindrical shells under axial compression. Journal of the Aeronautical Sciences, 8(8), 303-312

Lampinen, B. E., & Jeryan, R. A. (1982). Effectiveness of polyurethane foam in energy absorbing structures (No. 820494). SAE Technical Paper.

Liu, S., Tong, Z., Tang, Z., Liu, Y., & Zhang, Z. (2015). Bionic design modification of non-convex multi-corner thin-walled columns for improving energy absorption through adding bulkheads. Thin Walled Structures, 88, 70–81.

NDT Resource Center. (n.d.). Materials and Processes: Tensile Properties. [online] Available at: https://www.ndeed.org/EducationResources/CommunityCollege/Materials/Mechanical/Tensile.htm [Accessed on 9 December 2016].

Pugsley, A. G. (1979). On the crumpling of thin tubular struts. The Quarterly Journal of Mechanics and Applied Mathematics, 32(1), 1-7.

Pugsley, Sir A. and Macaulay, M (1960) The large scale crumpling of thin cylindrical colums. Quart. J. Mech. Appl. Math. 13, 1-9.

Reddy, T. Y., & Wall, R. J. (1988). Axial compression of foam-filled thin-walled circular tubes. International Journal of Impact Engineering, 7(2), 151-166.

Reddy, T. Y., & Al-Hassani, S. T. S. (1993). Axial crushing of wood-filled square metal tubes. International Journal of Mechanical Sciences, 35(3–4), 231–246.

Reid, S. R., Reddy, T. Y., & Gray, M. D. (1986). Static and dynamic axial crushing of foam-filled sheet metal tubes. International Journal of Mechanical Sciences, 28(5), 295-322.

Seitzberger, M., Rammerstorfer, F. G., Gradinger, R., Degischer, H. P., Blaimschein, M., & Walch, C. (2000). Experimental studies on the quasi-static axial crushing of steel columns filled with aluminium foam. International Journal of Solids and Structures, 37, 4125–4147.

Singace, A.A. (1999) Axial crushing analysis of tubes deforming in the multi-lobe mode. Int. J. Mech. Sci.41, 865-90.

Thornton, P. H., Mahmood, H. F., & Magee, C. L. (1983). Energy absorption by structural collapse. Structural crashworthiness, 96-117.

Zaborski, A. (n.d.) Handouts for Afghans: Tensile test. [online]. Available at: http://limba.wil.pk.edu.pl/~az/tmp/tensile_test.pdf [Accessed on 8 December 2016].

APPENDIX A

APPENDIX A1

Table A1 Gantt chart for PSM 1

Task	**Week**													
	1	2	3	4	5	6	7	8	9	10	11	12	13	14
Final Year Project Briefing	■													
Literature Survey		■	■	■	■	■	■	■	■	■	■	■	■	■
Preparation and Submission of Progress Report						■								
Preparation for Material									■	■				
Conduct Tensile Test											■	■		
Draft Final Report													■	■

APPENDIX A2

Table A2 Gantt chart for PSM 2

Task	**Week**													
	1	2	3	4	5	6	7	8	9	10	11	12	13	14
Literature Survey														
Comparison Experimental Work with Theoretical														
Conduct Quasi-static Loading Test														
Analysis & Interpretation of Results														
Preparation of Final Report														
Submission and Presentation of Report														

APPENDIX B

APPENDIX B1

Figure B1 Deformation of 50mm wood-filled circular tube


4mm


8mm


12mm


16mm


20mm


24mm

APPENDIX B2

Figure B2 Deformation of 50mm circular hollow tube

4mm

8mm

12mm

16mm

20mm

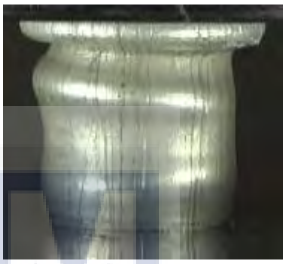

24mm

28mm

32mm

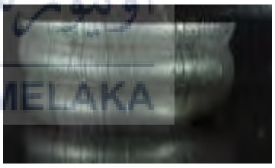

36mm

APPENDIX B3

Figure B3 Deformation of 50mm square hollow tube

4mm

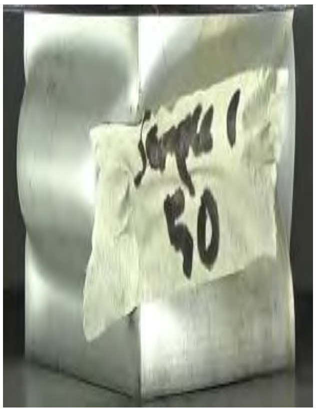

8mm

12mm

16mm

20mm

24mm

28mm

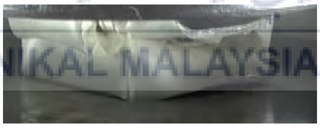

32mm

APPENDIX B4

Figure B4 Deformation of 50mm wood-filled square tube

4mm

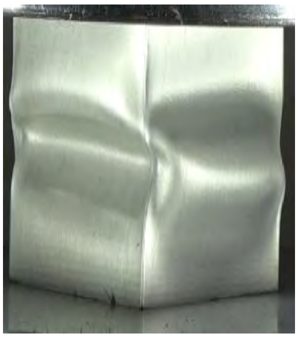

8mm

12mm

16mm

20mm

24mm

28mm

32mm

36mm

APPENDIX C

APPENDIX C1

Figure C1 Results of compression test for 50mm circular hollow tube

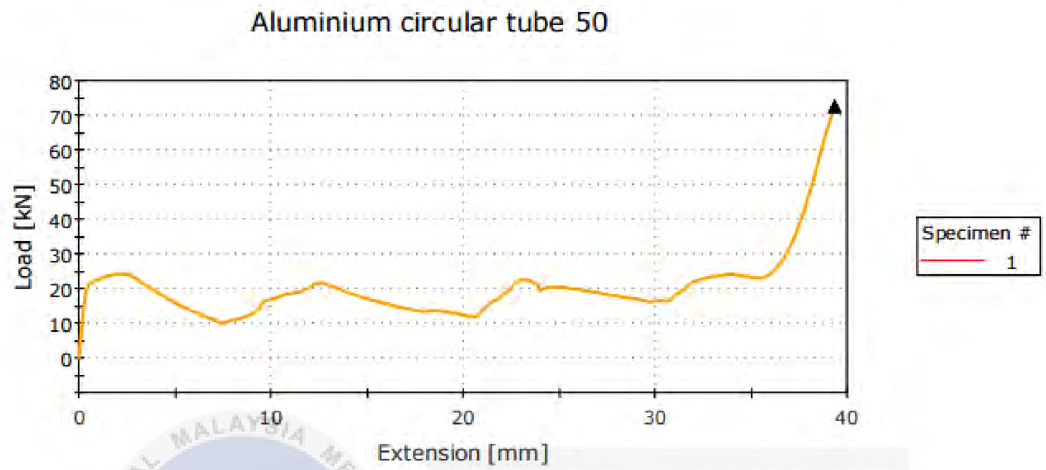

	Max Load [kN]	Compressive stress at Maximum Load [MPa]	Compressive strain (Extension) at Maximum Load [mm/mm]	Compressive extension at Maximum Load [mm]
1	> 72.5850	> 647.19	> 0.79	> 39.30

	Area under curve [J]	Energy at Maximum Compressive stress [J]	Load at Yield (Offset 0.2 %) [kN]	Compressive stress at Yield (Offset 0.2 %) [MPa]
1	-----	801.63	-----	-----

APPENDIX C2

Figure C2 Results of compression test for 50mm wood-filled circular tube

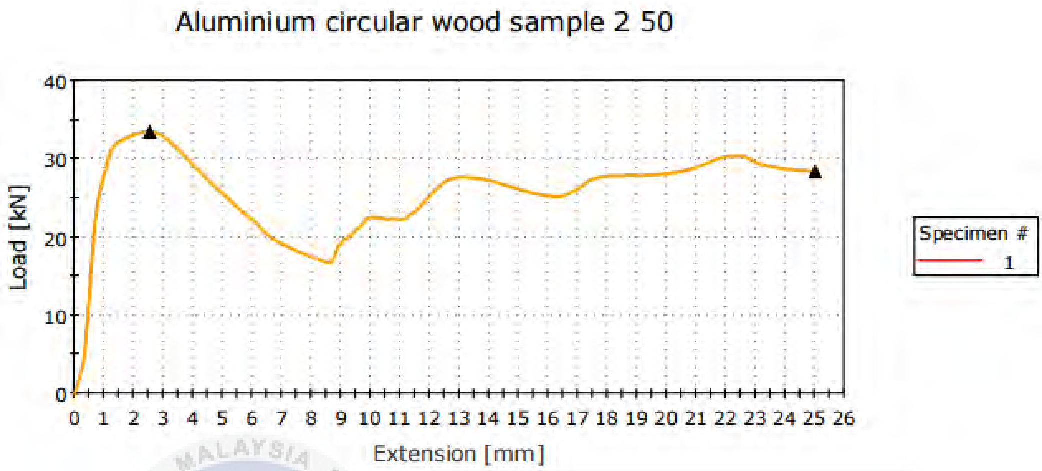

	Max Load [kN]	Compressive stress at Maximum Load [MPa]	Compressive strain (Extension) at Maximum Load [mm/mm]	Compressive extension at Maximum Load [mm]
1	> 33.3877	> 297.69	> 0.05	> 2.57

	Area under curve [J]	Energy at Maximum Compressive stress [J]	Load at Yield (Offset 0.2 %) [kN]	Compressive stress at Yield (Offset 0.2 %) [MPa]
1	-----	63.06	-----	-----

APPENDIX C3

Figure C3 Results of compression test for 50mm square hollow tube

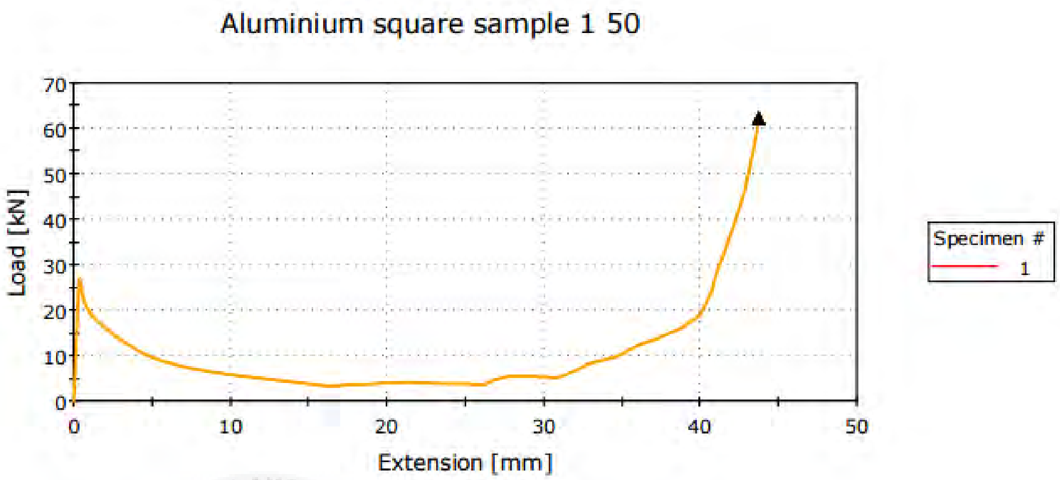

	Max Load [kN]	Compressive stress at Maximum Load [MPa]	Compressive strain (Extension) at Maximum Load [mm/mm]	Compressive extension at Maximum Load [mm]
1	> 62.2700	> 339.08	> 0.87	> 43.66

	Area under curve [J]	Energy at Maximum Compressive stress [J]	Load at Yield (Offset 0.2 %) [kN]	Compressive stress at Yield (Offset 0.2 %) [MPa]
1	-----	452.15	-----	-----

APPENDIX C4

Figure C4 Results of compression test for 50mm wood-filled square tube

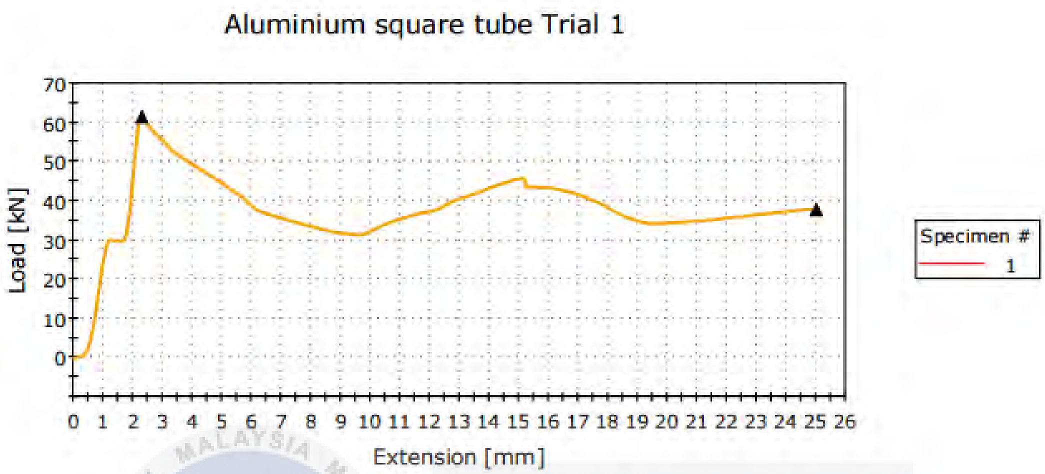

	Max Load [kN]	Compressive stress at Maximum Load [MPa]	Compressive strain (Extension) at Maximum Load [mm/mm]	Compressive extension at Maximum Load [mm]
1	> 61.34	> 30.77	> 0.05	> 2.33

	Area under curve [J]	Energy at Maximum Compressive stress [J]	Load at Yield (Offset 0.2 %) [kN]	Compressive stress at Yield (Offset 0.2 %) [MPa]
1	-----	55.06	-----	-----